Numerical schemes for kinetic equation with diffusion limit and anomalous time scale

Helene Hivert

Manuscript submitted to
AIMS' Journals
Volume **X**, Number **0X**, XX **200X**

doi:10.3934/xx.xx.xx.xx

pp. **X–XX**

NUMERICAL SCHEMES FOR KINETIC EQUATION WITH DIFFUSION LIMIT AND ANOMALOUS TIME SCALE

Hivert Hélène*

ENS Lyon, UMPA UMR 5669 CNRS, and Inria Rhône-Alpes, projet NUMED
46, allée d'Italie
69364 Lyon Cedex 07, FRANCE

(Communicated by the associate editor name)

Abstract. In this work, we propose numerical schemes for linear kinetic equation, which are able to deal with a diffusion limit and an anomalous time scale of the form $\varepsilon^2(1+|\ln(\varepsilon)|)$. When the equilibrium distribution function is a heavy-tailed function, it is known that for an appropriate time scale, the mean-free-path limit leads either to diffusion or fractional diffusion equation, depending on the tail of the equilibrium. The bifurcation between these two limits is the classical diffusion limit with anomalous time scale treated in this work. Our aim is to develop numerical schemes which work for the different regimes, with no restriction on the numerical parameters. Indeed, the degeneracy $\varepsilon \to 0$ makes the kinetic equation stiff. From a numerical point of view, it is necessary to construct schemes able to undertake this stiffness to avoid the increase of computational cost. In this case, it is crucial to capture numerically the effects of the large velocities of the heavy-tailed equilibrium. Since the degeneracy towards the diffusion limit is very slow, it is also essential to respect the asymptotic behavior of the solution, and not only the limit. Various numerical tests are performed to illustrate the efficiency of our methods in this context.

1. **Introduction.** The modeling of a large amount of particles, from a theoretical or numerical point of view, is a very active field of research. The direct application of Newton's laws leads to a large system of coupled equations, one for each particle of the system. Since such a huge number of unknowns is beyond the reach of numerical computations, the so-called microscopic scale is not adapted to the numerical analysis of these systems. Instead, an approach based on statistical physics is preferred, where the distribution function of particles $f_\varepsilon(t,x,v)$ depending on the time $t \geq 0$, the position $x \in \mathbb{R}^d$, and the velocity $v \in \mathbb{R}^d$ is considered. The parameter $\varepsilon \in (0,1]$ denotes here the Knudsen number, which is proportional to the mean free path of the particle.

Provided an initial condition $f(0,x,v) = f_{in}(x,v)$, we consider the following kinetic equation for f_ε

$$\Theta(\varepsilon)\partial_t f_\varepsilon + \varepsilon v \cdot \nabla_x f_\varepsilon = L(f_\varepsilon). \tag{1}$$

2010 *Mathematics Subject Classification.* Primary: 35B40, 65L04, 41A60 ; Secondary: 65M22.

Key words and phrases. BGK equation, anomalous diffusion limit, multiscale scheme, asymptotic preserving scheme, asymptotic analysis.

The author is supported by ERC starting grant MESOPROBIO.

* Corresponding author.

The quantity $\Theta(\varepsilon) = \varepsilon^2 (1 + \ln(\varepsilon))$, is a suitable scaling parameter to be chosen according to the nature of L, in order to capture a non-trivial dynamic when ε goes to 0. The linear operator L describes the collisions of the particles. We will consider the particular case of the BGK operator

$$L(f_\varepsilon) = \rho_\varepsilon M - f_\varepsilon, \tag{2}$$

with

$$\rho_\varepsilon(t,x) = \int_{\mathbb{R}^d} f_\varepsilon(t,x,v)\mathrm{d}v =: \langle f_\varepsilon \rangle (t,x).$$

Here, the equilibrium function M is even, positive and normalized to 1

$$M(-v) = M(v) > 0 \quad \text{for all} \quad v \in \mathbb{R}^d \quad \text{and} \quad \langle M \rangle = 1.$$

In what follows, the integral in v of f on a domain $\mathcal{D}$ will always be denoted $\langle f \rangle_{\mathcal{D}}$. The integral is on the whole space $\mathbb{R}^d$ when no domain is specified.

The asymptotic analysis of (1) when $\varepsilon \to 0$ can be found in [27]. Our aim in this paper is to construct numerical schemes for (1) that fit with this asymptotic analysis. The properties of the equilibrium function M, and the scaling $\Theta(\varepsilon)$ of (1) make various asymptotic behaviors arise. For instance, considering the scaling $\Theta(\varepsilon) = \varepsilon$ with a local Maxwellian equilibrium in (1) and the Boltzmann operator instead of the linear collision operator L, leads when ε goes to 0 to a fluid limit for (1) (see [1, 2]). With the BGK collision operator, the scaling $\Theta(\varepsilon) = \varepsilon^2$, and a global Maxwellian equilibrium $M(v) = (2\pi)^{-d/2}\mathrm{e}^{-v^2/2}$, the solution f_ε of (1) degenerates when $\varepsilon \to 0$ to a distribution at equilibrium $f = \rho M$, where ρ solves a diffusion equation

$$\partial_t \rho - \nabla_x \cdot (D \nabla_x \rho) = 0,$$

with initial condition $\rho_{in} = \langle f_{in} \rangle$. A rigorous derivation of diffusion-type equations in this last case was first investigated in [31, 3, 5, 15]. When M is a Maxwellian and $\Theta(\varepsilon) = \varepsilon^2$, the diffusion coefficient D is finite because of the exponential decay of M for large v, and is given by

$$D = \langle v \otimes v M \rangle . \tag{3}$$

However, for non Maxwellian equilibrium, it may happen in many situations that the coefficient D becomes infinite. An important example is the case of a so-called heavy-tailed function $M(v) \sim 1/|v|^{d+\alpha}$ for large v, $\alpha \in (0,2)$. In this case, the scaling $\Theta(\varepsilon) = \varepsilon^2$ is not the suitable choice and does not lead to a non trivial dynamics when ε goes to 0. It is well-known that, in this case, the time scale $\Theta(\varepsilon)$ should be modified according to α in order to capture a non-trivial dynamics, which turns out to be a fractional diffusion model [27, 4]. Heavy-tailed equilibria arise in the study of granular media (see [17, 7, 6]), astrophysical plasmas (see [28, 29]), tokamaks (see [16]) or in economy (see [23]). Usually, the fractional diffusion equation describes the motion of the particles driven by a Levy process (see [14, 13]), while the classical diffusion is governed by a Brownian process.

From a numerical point of view, the case $\alpha \in (0,2)$ has been treated in [11, 10, 30]. In this paper, we consider the so-called critical case $\alpha = 2$, of the above heavy-tailed equilibrium, which induces a different asymptotic behavior when ε goes to 0. For a sake of simplicity we will consider here the following particular case

$$M(v) = \begin{cases} m & |v| < 1 \\ m/|v|^{d+2} & |v| \geq 1, \end{cases} \tag{4}$$

where m is such that $\langle M\rangle = 1$. With this assumption, it has been shown in [27] that if $\Theta(\varepsilon) \sim \varepsilon^2|\ln(\varepsilon)|$ in (1) the solution f_ε of (1) converges weakly when $\varepsilon \to 0$ to $\rho_0 M$, where ρ_0 solves a classical diffusion equation

$$\begin{cases} \partial_t \rho_0 - c_d m \Delta \rho_0 = 0, \\ \rho_0(0,x) = \rho_{in}(x) = \langle f_{in}\rangle(x). \end{cases} \tag{5}$$

Here c_d is a coefficient that only depends on the dimension d ($c_1 = 2, c_2 = \pi$, and $c_3 = 8\pi/3$). To have a non-vanishing of $\Theta(\varepsilon)$ for $\varepsilon = 1$, we shall consider

$$\Theta(\varepsilon) = \varepsilon^2\left(1 + |\ln(\varepsilon)|\right). \tag{6}$$

In this work, we prove that when the initial data f_{in} is at equilibrium, the convergence when $\varepsilon \to 0$ of the solution f_ε of (1) to the solution of (5) is very slow. However, we will show that f_ε approaches much faster an intermediate equilibrium $\tilde\rho_\varepsilon M$, where $\tilde\rho_\varepsilon$ is the solution of the following equation (in Fourier variable)

$$\begin{cases} \partial_t \hat{\tilde\rho}_\varepsilon + a_\varepsilon(k)\hat{\tilde\rho}_\varepsilon = 0, & t > 0, k \in \mathbb{R}^d \\ \hat{\tilde\rho}_\varepsilon(0,k) = \hat\rho_{in}(k), & k \in \mathbb{R}^d, \end{cases} \tag{7}$$

and

$$a_\varepsilon(k) = \frac{1}{\Theta(\varepsilon)}\left\langle \frac{\varepsilon^2(k\cdot v)^2}{1+\varepsilon^2(k\cdot v)^2} M \right\rangle, \tag{8}$$

where $\hat{\tilde\rho}_\varepsilon$ is the space Fourier transform of $\tilde\rho_\varepsilon$.

The main goal of this work is to construct numerical schemes for (1) which do not need to be refined in order to capture the right asymptotic behavior, when ε goes to 0. There are, in fact, some stiffness in the problem (1). First, the smallness of ε imposes severe conditions on the numerical parameters, if a naive approach is used. We will follow an *Asymptotic Preserving* (AP) strategy [18, 21, 22] to overcome this difficulty. Namely, if we consider a problem P_ε which degenerates into a problem P_0 when ε tends to 0, then an AP scheme S^h_ε should enjoy the following properties:

1. at fixed ε, S^h_ε must be consistent with P_ε when the discretization parameter h tends to 0.
2. S^h_ε must degenerate into a scheme S^h_0 consistent with P_0 when ε goes to 0.

An AP scheme can even enjoy the stronger property of being *Uniformly Accurate* (UA), meaning that its accuracy does not depend on ε.

The construction of AP schemes for the case of classical diffusion with classical time scale $\Theta(\varepsilon) = \varepsilon^2$ has been widely investigated (see [18, 19, 19, 20, 21, 8, 9, 26, 25]), but the heavy-tail of the equilibrium brings an additional stiffness, which is not usual in the classical cases. Indeed, the anomalous time scale (6) in (1) is designed to capture the effect of the high velocities in the asymptotic analysis. From a numerical point of view, taking into account these high velocities is then crucial to ensure the AP property of the scheme. In previous works (see [10, 11, 12]), we investigated AP schemes for kinetic equations in the fractional diffusion limit. In the critical case, the same methodology can not be applied since the resulting schemes do not respect the dynamics of the convergence towards the diffusion equation (1). This is due to the slow convergence in this critical case, and a specific study will be performed to capture the right asymptotic behavior.

Three numerical schemes will be investigated in this paper. The first one is based on a fully implicit in time scheme for (1) using a Fourier variable in space. A suitable modification is introduced in this case, and its AP behavior is proved. Then, a scheme based on a micro-macro decomposition of the distribution function

f_ε is presented. It allows to avoid, if needed, the use of the Fourier transform and of the time implicit character of the previous scheme. Moreover, it can be adapted to deal with more general collision operators in (1). Once again, the convergence towards (7) has to be treated with care to ensure the good asymptotic behavior of the scheme. Eventually, we propose an approach based on an integral formulation of (1) in Fourier variable, which enjoys the stronger UA property.

To summarize, we will show that (1) approaches (7) with a rate $\varepsilon\sqrt{1+|\ln(\varepsilon)|}$, while (7) approaches the limit model (5) with the slower rate $1/\left(1+|\ln(\varepsilon)|\right)$, and we will construct numerical schemes which respect this asymptotic behavior. This can be illustrated by the following diagram

$$\begin{array}{ccccc} P_\varepsilon : (1) & \xrightarrow[\varepsilon\sqrt{1+|\ln(\varepsilon)|}]{} & \tilde{P}_\varepsilon : (7) & \xrightarrow[1/(1+|\ln(\varepsilon)|)]{} & P_0 : (5) \\ \uparrow{\scriptstyle h\to 0} & & \uparrow{\scriptstyle h\to 0} & & \uparrow{\scriptstyle h\to 0} \\ S_\varepsilon^h & \xrightarrow[\varepsilon\sqrt{1+|\ln(\varepsilon)|}]{} & \tilde{S}_\varepsilon^h & \xrightarrow[1/(1+|\ln(\varepsilon)|)]{} & S_0^h \end{array} \tag{9}$$

The schemes S_ε^h and $\tilde{S}_\varepsilon^h$ are respectively consistent with the problems P_ε and $\tilde{P}_\varepsilon$ when $\varepsilon > 0$ is fixed, and S_0^h is consistent with P_0. The scheme S_ε^h approaches $\tilde{S}_\varepsilon^h$ with rate $\varepsilon\sqrt{1+|\ln(\varepsilon)|}$ while $\tilde{S}_\varepsilon^h$ approaches S_0 with rate $1/\left(1+|\ln(\varepsilon)|\right)$ when the discretization parameter h is fixed and when ε goes to 0. The asymptotic behavior $P_\varepsilon \to \tilde{P}_\varepsilon \to P_0$ will be proved in suitable functional spaces and illustrated by several numerical tests.

The paper is organized as follows. In the next section, we will start by establishing the convergence rates of (1) towards (5), and of (7) to (5). Then, in Section 3, we present an asymptotic preserving scheme for (7), and the three asymptotic preserving schemes for (1), which are tested in Section 4.

2. Degeneracy to the diffusion limit.

In this section, we show that the convergence of (1) towards the diffusion limit (5) can be quantified by two steps as described by the diagram (9). This will be the basis of the numerical methods proposed in Section 3. In what follows, the space Fourier transform will be often used. We will denote $\hat{f}(t,k,v)$ (resp. $\hat{\rho}(t,k)$) the space Fourier transform of $f(t,x,v)$ (resp. $\rho(t,x)$)

$$\hat{f}(t,k,v) = \int_{\mathbb{R}^d} \mathrm{e}^{-ik\cdot x} f(t,x,v)\mathrm{d}x.$$

We will use the following weighted L^2 norm

$$\|f(x,v)\|^2_{L^2_{M^{-1}}} = \int_{\mathbb{R}^d}\int_{\mathbb{R}^d} |f(x,v)|^2 \frac{1}{M(v)}\mathrm{d}v\mathrm{d}x, \tag{10}$$

where M is given by (4). We have the following propositions:

Proposition 1. *Let $f_\varepsilon \in L^\infty\left(0,T;L^2_{M^{-1}}\right)$ be the solution of (1) with initial condition $f_{in}(x,v) = \rho_{in}(x)M(v)$, with $\rho_{in} \in H^{N_d}\left(\mathbb{R}^d\right)$ ($N_1 = 3, N_2 = N_3 = 6$), where $H^{N_d}\left(\mathbb{R}^d\right)$ denotes the usual Sobolev space, and let $T > 0$. Then, there exists a constant C such that*

$$\|f_\varepsilon - \tilde{\rho}_\varepsilon M\|_{L^\infty\left(0,T;L^2_{M^{-1}}\right)} \leq CT\varepsilon\sqrt{1+|\ln(\varepsilon)|}\|\rho_{in}\|_{H^{N_d}}, \tag{11}$$

where $\tilde{\rho}_\varepsilon \in L^\infty\left(0,T;L^2\right)$ *solves* (7) *with initial condition* ρ_{in}*, and with* M *defined in* (4)*.*

Proposition 2. *Assume that the previous assumptions hold, and let* $\tilde{\rho}_\varepsilon \in L^\infty\left(0,T;L^2(\mathbb{R}^d)\right)$ *be the solution of* (7) *with* $\rho_{in} \in H^{M_d}\left(\mathbb{R}^d\right)$ *(*$M_1 = 2$*,* $M_2 = M_3 = 4$*), and let* $T > 0$*. Then, there exists a constant* C *such that*

$$\|\tilde{\rho}_\varepsilon - \rho_0\|_{L^\infty(0,T;L^2(\mathbb{R}^d))} \leq \frac{CT}{1+|\ln(\varepsilon)|}\|\rho_{in}\|_{H^{M_d}}, \tag{12}$$

where $\rho_0 \in L^\infty\left(0,T;L^2(\mathbb{R}^d)\right)$ *solves* (5)*, with initial condition* ρ_{in}*.*

These two propositions establish that the convergence $\varepsilon \to 0$ of (1) makes appear two dynamics with very different rates in ε. Indeed, in a first step, the solution f_ε approaches (relatively) quickly a distribution function at equilibrium $\tilde{\rho}_\varepsilon(t,x)M(v)$, with $\tilde{\rho}_\varepsilon$ solution of (7). Then, in a second step, this density $\tilde{\rho}_\varepsilon$ goes much more slowly to the solution ρ_0 of the limit diffusion equation (5). Hence, the approximation of f_ε by its diffusion limit (5) is valid only for very small ε. At the numerical level, it implies that a large range of ε may stay out of reach if no appropriate strategy is used in the numerical schemes. The next parts present numerical methods for (1) degenerating when ε to 0 into numerical methods solving (7). In particular, the schemes enjoy the AP property that is

- when ε is fixed, the scheme is consistent with (1),
- the difference between the numerical scheme S_ε^h for (1) and the numerical scheme $\tilde{S}_\varepsilon^h$ for (7) converges to 0 when ε goes to 0.

Afterwards, letting ε go to zero in the scheme $\tilde{S}_\varepsilon^h$ for (7) makes it degenerate in a scheme S_0^h solving the limit diffusion equation (5). This approach enables to capture numerically the two scales of convergence of the solution of (1) to its diffusion limit, as described by (9).

The proofs of Prop. 1 and Prop. 2 follows the ideas developed in [4] in the case of a fractional diffusion limit for kinetic equation, coming from a heavy-tailed equilibrium function. We start by proving the following lemma, which gives the limit of a_ε when ε goes to 0.

Lemma 2.1. *Considering* a_ε *defined in* (8)*, there exists a constant* C *such that,* $\forall k \in \mathbb{R}^d$

1. *If* $d = 1$*,*

$$\left|a_\varepsilon(k) - 2mk^2\right| \leq \frac{C}{1+|\ln(\varepsilon)|}\left(1+k^2\right). \tag{13}$$

2. *If* $d = 2, 3$*,*

$$|a_\varepsilon(k) - c_d m|k|^2| \leq \frac{C}{1+|\ln(\varepsilon)|}\left(1+|k|^4\right) \tag{14}$$

with $c_2 = \pi$ *and* $c_3 = \frac{8\pi}{3}$*.*

Proof of Lemma 2.1. In the 1-dimensional case, with the change of variables $w = \varepsilon v$, the coefficient a_ε reads

$$a_\varepsilon(k) = \frac{m}{1+|\ln(\varepsilon)|}\left\langle \frac{k^2v^2}{1+\varepsilon^2k^2v^2}\right\rangle_{|v|<1} + \frac{m}{1+|\ln(\varepsilon)|}\left\langle \frac{k^2w^2}{1+k^2w^2}\frac{1}{|w|^3}\right\rangle_{|w|\geq\varepsilon}, \tag{15}$$

where the last term in (15) can be computed for nonzero k with the change of variables $u = 1/w$

$$\frac{m}{1+|\ln(\varepsilon)|}\left\langle \frac{k^2w^2}{1+k^2w^2}\frac{1}{|w|^3}\right\rangle_{|w|\geq\varepsilon} = 2mk^2 + \frac{2mk^2}{1+|\ln(\varepsilon)|}\left(\frac{1}{2}\ln\left(\varepsilon^2+\frac{1}{k^2}\right)-1\right),$$

and the first term is bounded by $Ck^2/(1+|\ln(\varepsilon)|)$. Eventually the inequality $\ln(x)/2 \leq 1+x$ for $x>0$, gives (13).

When $d = 2, 3$, with the change of variables $w = \varepsilon|k|v$ for nonzero k, (8) reads

$$a_\varepsilon(k) = \frac{m}{1+|\ln(\varepsilon)|}\left\langle \frac{(k\cdot v)^2}{1+\varepsilon^2(k\cdot v)^2}\right\rangle_{|v|\leq 1} + \frac{m|k|^2}{1+|\ln(\varepsilon)|}\left\langle \frac{(w\cdot e)^2}{1+(w\cdot e)^2}\frac{1}{|w|^{d+2}}\right\rangle_{|w|\geq\varepsilon|k|}, \tag{16}$$

where e denotes any unitary vector. The first term is lower than $C|k|^2$, it remains to consider the second one. Depending on the dimension, a change of variables in polar or spherical coordinates can be applied in it. Since no additional difficulty arise when $d = 3$, we treat here the case of polar coordinates, when $d = 2$. Choosing e such that $w \cdot e = |w|\cos(\theta)$, it can be rewritten as

$$\left\langle \frac{(w\cdot e)^2}{1+(w\cdot e)^2}\frac{1}{|w|^{d+2}}\right\rangle_{|w|\geq\varepsilon|k|} = I_1 + I_2 + I_3,$$

with

$$I_1 = \int_{\theta=0}^{2\pi}\int_{r=\varepsilon|k|}^{1} r^2\cos^2(\theta)\frac{1}{r^3}\mathrm{d}r\mathrm{d}\theta, \tag{17}$$

$$I_2 = \int_{\theta=0}^{2\pi}\int_{r=\varepsilon|k|}^{1} r^2\cos^2(\theta)\left(\frac{1}{1+r^2\cos^2(\theta)}-1\right)\frac{1}{r^3}\mathrm{d}r\mathrm{d}\theta \tag{18}$$

$$I_3 = \int_{\theta=0}^{2\pi}\int_{r=1}^{\infty} \frac{r^2\cos^2(\theta)}{1+r^2\cos^2(\theta)}\frac{1}{r^3}\mathrm{d}r\mathrm{d}\theta. \tag{19}$$

At this stage, the last two integrals can be bounded

$$|I_2| \leq \int_{\theta=0}^{2\pi}\int_{r=\varepsilon|k|}^{1}\frac{r^4\cos^4(\theta)}{1+r^2\cos^2(\theta)}\frac{1}{r^3}\mathrm{d}r\mathrm{d}\theta \leq \int_{\theta=0}^{2\pi}\int_{r=\varepsilon|k|}^{1} r\cos^4(\theta)\mathrm{d}r\mathrm{d}\theta \leq C(1+|k|^2)$$

$$|I_3| \leq \int_{0}^{2\pi}\int_{r=1}^{\infty}\frac{1}{r^3}\mathrm{d}r\mathrm{d}\theta \leq C,$$

and the first one can be computed explicitly

$$I_1 = -\pi\ln(|k|) - \pi\ln(\varepsilon).$$

Eventually, the inequality $\ln(|k|) \leq |k|$ yields (14). □

Remark 1. The proof of Lemma 2.1 provides, for nonzero k, a rewriting of a_ε in which the diffusion limit clearly appears. In dimension 1, it is

$$\begin{aligned} a_\varepsilon^{d=1}(k) = 2mk^2 &+ \frac{m}{1+|\ln(\varepsilon)|}\left\langle \frac{k^2v^2}{1+\varepsilon^2k^2v^2}\right\rangle_{|v|<1} \\ &+ \frac{2mk^2}{1+|\ln(\varepsilon)|}\left(\frac{1}{2}\ln\left(\varepsilon^2+\frac{1}{k^2}\right)-1\right), \end{aligned} \tag{20}$$

and in dimension 2 it reads

$$a_\varepsilon^{d=2}(k) = \pi m|k|^2 + \frac{m}{1+|\ln(\varepsilon)|}\left\langle \frac{(k\cdot v)^2}{1+\varepsilon^2(k\cdot v)^2}\right\rangle_{|v|\geq 1} - \frac{m|k|^2}{1+|\ln(\varepsilon)|}\pi\left(1+\ln(|k|)\right) - \frac{m|k|^2}{1+|\ln(\varepsilon)|}\int_{\theta=0}^{2\pi}\int_{r=\varepsilon|k|}^{1}\frac{r\cos^4(\theta)}{1+r^2\cos^2(\theta)}\mathrm{d}r\mathrm{d}\theta + \frac{m|k|^2}{1+|\ln(\varepsilon)|}\int_{\theta=0}^{2\pi}\int_{r=1}^{\infty}\frac{\cos^2(\theta)}{1+r^2\cos^2(\theta)}\frac{1}{r}\mathrm{d}r\mathrm{d}\theta. \tag{21}$$

Eventually, a change of variables in spherical coordinates provides the case of dimension 3

$$a_\varepsilon^{d=3}(k) = \frac{8\pi}{3}m|k|^2 + \frac{m}{1+|\ln(\varepsilon)|}\left\langle \frac{(k\cdot v)^2}{1+\varepsilon^2(k\cdot v)^2}\right\rangle_{|v|\geq 1} - \frac{m|k|^2}{1+|\ln(\varepsilon)|}\frac{8\pi}{3}\left(\ln(|k|)+1\right) - \frac{2\pi m|k|^2}{1+|\ln(\varepsilon)|}\int_{\theta=0}^{\pi}\int_{r=\varepsilon|k|}^{1}\frac{r\sin^5(\theta)}{1+r^2\sin^2(\theta)}\mathrm{d}r\mathrm{d}\theta + \frac{2\pi m|k|^2}{1+|\ln(\varepsilon)|}\int_{\theta=0}^{\pi}\int_{r=1}^{\infty}\frac{\sin^2(\theta)}{1+r^2\sin^2(\theta)}\frac{1}{r}\mathrm{d}r\mathrm{d}\theta. \tag{22}$$

Proof of Prop. 2. We denote by $\hat\rho_0$ and $\hat{\tilde\rho}_\varepsilon$ the solutions of (5) and (7) in space Fourier variable, with initial condition $\hat\rho_{in}$, and $a_0(k) = c_d m k^2$. They satisfy

$$\hat{\tilde\rho}_\varepsilon(t,k) = \mathrm{e}^{-t a_\varepsilon(k)}\hat\rho_{in}(k),$$
$$\hat\rho_0(t,k) = \mathrm{e}^{-t a_0(k)}\hat\rho_{in}(k).$$

Since $a_\varepsilon(k)\geq 0$ and $a_0(k)\geq 0$, the inequality $|\mathrm{e}^{-x}-\mathrm{e}^{-y}|\leq |x-y|$ for $x\geq 0, y\geq 0$ yields

$$\begin{cases} |\hat\rho_0 - \hat{\tilde\rho}_\varepsilon| \leq \dfrac{Ct}{1+|\ln(\varepsilon)|}\left(1+k^2\right)|\hat\rho_{in}| & \text{if } d=1, \\ |\hat\rho_0 - \hat{\tilde\rho}_\varepsilon| \leq \dfrac{Ct}{1+|\ln(\varepsilon)|}\left(1+|k|^2\right)^2|\hat\rho_{in}| & \text{if } d=2,3, \end{cases}$$

and gives (12). □

The convergence of the solution of (7) to the solution of (5) is very slow in ε, but Prop. 1 states that the degeneracy of (1) to (7) happens much faster. The proof of Prop. 1 is based on the proof of the similar result stated in [4] for the case of a kinetic equation with heavy-tailed equilibrium degenerating to a fractional diffusion equation. It uses the following properties of the collision operator, established in [15] and [27] in a more general case:

Proposition 3. *The collision operator L given by (2) has the following properties*

1. *The operator L is bounded in $L^2_{M^{-1}}(\mathbb{R}^d\times\mathbb{R}^d)$.*
2. *There exists a constant $C>0$ such that*
$$\forall f\in L^2_{M^{-1}},\ \int_{\mathbb{R}^d} L(f)\frac{f}{M}\mathrm{d}v \leq -\frac{1}{2}\int_{\mathbb{R}^d}|f-\langle f\rangle M|^2\frac{1}{M}\mathrm{d}v.$$
3. *For $h\in L^2_{M^{-1}}$, the equation $L(g)=h$ has a solution if and only if $\langle h\rangle = 0$. If $\langle g\rangle = 0$, this solution is unique.*

Proof of Prop. 1. As in [4], the proof relies on the following Hilbert expansion of the solution f_ε of (1)

$$f_\varepsilon = \tilde{\rho}_\varepsilon M + g_1 + g_2 + r,$$

where ρ, g_1, g_2 and r solve

$$(1 + \varepsilon v \cdot \nabla_x)\, g_1 = -\varepsilon v \cdot \nabla_x \tilde{\rho}_\varepsilon M \tag{23}$$

$$\langle g_2 \rangle\, M - g_2 = -\langle g_1 \rangle\, M + \Theta(\varepsilon)\partial_t \tilde{\rho}_\varepsilon M \tag{24}$$

$$\partial_t r + \frac{\varepsilon}{\Theta(\varepsilon)} v \cdot \nabla_x r = \frac{1}{\Theta(\varepsilon)} \left(\langle r \rangle\, M - r\right) - \partial_t g_1 - \left(\partial_t g_2 + \frac{\varepsilon}{\Theta(\varepsilon)} v \cdot \nabla_x g_2\right) \tag{25}$$

with initial condition $\tilde{\rho}_\varepsilon(0,x) = \rho_{in}(x), g_1(0,x,v) = g_2(0,x,v) = r(0,x,v) = 0$. Considering (23) in Fourier variable leads to

$$\hat{g}_1 = -\frac{\mathrm{i}\varepsilon k \cdot v}{1 + \mathrm{i}\varepsilon k \cdot v} \hat{\tilde{\rho}}_\varepsilon M. \tag{26}$$

Furthermore, the left-hand side of (24) is such that $\langle \langle g_2 \rangle\, M - g_2 \rangle = 0$. Still in Fourier variable, (24) then reads $-\langle g_1 \rangle + \Theta(\varepsilon)\partial_t \tilde{\rho}_\varepsilon = 0$, that is using (26) and the symmetry of M

$$\partial_t \hat{\tilde{\rho}}_\varepsilon(t,k) + a_\varepsilon(k) \hat{\tilde{\rho}}_\varepsilon(t,k) = 0,$$

with a_ε defined in (8). Note that solving this equation leads to

$$\hat{\tilde{\rho}}_\varepsilon(t,k) = \mathrm{e}^{-a_\varepsilon(k)t} \hat{\rho}_{in}(k), \quad \partial_t \hat{\tilde{\rho}}_\varepsilon(t,k) = -a_\varepsilon(k) \mathrm{e}^{-a_\varepsilon(k)t} \hat{\rho}_{in}(k). \tag{27}$$

As $\hat{\rho}$ solves (7), the proof of the proposition relies on establishing estimates for $\|g_1\|_{L^\infty(0,T;L^2_{M^{-1}})}$, $\|g_2\|_{L^\infty(0,T;L^2_{M^{-1}})}$ and $\|r\|_{L^\infty(0,T;L^2_{M^{-1}})}$. Since $a_\varepsilon \geq 0$, (27) and the expression of $\hat{g}_1$ in (26) give

$$\int_{\mathbb{R}^d} |\hat{g}_1|^2 \frac{\mathrm{d}v}{M} \leq \Theta(\varepsilon) a_\varepsilon(k) |\hat{\rho}_{in}|^2,$$

with $\Theta(\varepsilon)$ defined in (6). The estimation of a_ε given by Lemma 2.1 yields

$$\|g_1\|_{L^\infty(0,T;L^2_{M^{-1}})} \leq C\varepsilon \sqrt{1 + |\ln(\varepsilon)|} \|\rho_{in}\|_{H^{N_d}}, \tag{28}$$

with $N_1 = 1$, and $N_2 = N_3 = 2$.

The solution g_2 of (24) is unique if $\langle g_2 \rangle = 0$. It can be rewritten as

$$-g_2 = -\langle g_1 \rangle\, M + \Theta(\varepsilon)\partial_t \tilde{\rho}_\varepsilon M,$$

and (26) and (7) imply $g_2 = 0$.

The estimation of r can be done with (25) integrated on the characteristic curves, multiplied by r/M and integrated in velocity. Since $g_2 = 0$ and the term in $\langle r \rangle\, M - r$ gives a negative integral with the second point of Prop. 3, it reads

$$\frac{1}{2} \frac{\mathrm{d}}{\mathrm{d}t} \int_{\mathbb{R}^d} \frac{r^2(t, X(t), v)}{M} \mathrm{d}v \leq -\int_{\mathbb{R}^d} \partial_t g_1\left(t, X(t), v\right) \frac{r(t, X(t), v)}{M} \mathrm{d}v,$$

where $X(t) = x + \frac{\varepsilon}{\Theta(\varepsilon)} tv$. After an integration in time and space, and using a Cauchy-Schwarz inequality, it eventually writes

$$\frac{1}{2} \|r\|_{L^\infty(0,T;L^2_{M^{-1}})} \leq \|\partial_t g_1\|_{L^1(0,T;L^2_{M^{-1}})},$$

so that an upper bound for the right-hand side is needed to complete the proof of the proposition. A differentiation in time of (26), together with (27), gives

$$\|\partial_t g_1\|^2_{L^2_{M^{-1}}} \leq \Theta(\varepsilon) \int_{\mathbb{R}^d} a_\varepsilon(k)^3 \mathrm{e}^{-a_\varepsilon(k)t} |\hat{\rho}_{in}|^2 \mathrm{d}k,$$

hence, using Lemma 2.1

$$\|\partial_t g_1\|_{L^1(0,T;L^2_{M^{-1}})} \leq CT\varepsilon\sqrt{1+|\ln(\varepsilon)|}\|\rho_{in}\|_{H^{N_d}},$$

which completes the proof. □

3. **Numerical schemes.** This section presents three numerical schemes designed to approximate the solution of (1), and to respect the asymptotic behavior of Prop. 1 and Prop. 2 when ε becomes small. These schemes are based respectively on an implicit formulation of (1) in Fourier variable, a micro-macro decomposition, and an integral formulation of (1). These three strategies have been investigated in [11, 12] in the case of the fractional diffusion limit of the kinetic equation, $\alpha \in (0,2)$. Here we extend them to the case $\alpha = 2$. In this critical case, we required that not only the limit equation (5), but the asymptotic behavior (7) of the numerical solution is prescribed.

In what follows, we will denote by $t_n = n\Delta t, 0 \leq n \leq N$, such that $N\Delta t = T$ the time discretization, and we will set $f^n \approx f(t_n)$. All the numerical tests will be performed at time $T = 0.1$, the time step Δt being specified in each case. The schemes require a velocity discretization, we will denote

$$\langle f \rangle_{N_v,D} = \Delta v \sum_{\substack{j=1 \\ v_j \in D}}^{N_v} f(v_j), \tag{29}$$

the quadrature formula for the integration in velocity on the domain D. When no domain is specified, the integration is for all the index $1 \leq j \leq N_v$. In the tests, we will consider a uniform discretization of the domain $|v| \leq 10$, with N_v points symmetrically distributed on both sides of the origin to ensure that $\langle vM \rangle_{N_v} = 0$. Namely, we will consider $N_v = 2N_v'$ with $N_v' = 100$ and use the grid

$$v_j = -10 + \frac{\Delta v}{2} + (j-1)\Delta v, \quad 1 \leq j \leq 2N_v', \tag{30}$$

with $\Delta v = 10/N_v'$. The normalization constant m of the equilibrium M is chosen such that $\langle M \rangle_{N_v} = 1$. The space domain is bounded, and we consider periodic conditions, allowing the use of the Fourier variable. At the discrete level, the discrete Fourier variable will be used. In the tests, we will consider $x \in [-1,1]$, discretized with N_x points such that

$$x_i = -1 + (i-1)\Delta x, \quad 1 \leq i \leq N_x, \tag{31}$$

where $\Delta x = 2/N_x$. This space discretization is linked to the Fourier modes we use for the computation of the discrete Fourier transform, that are the integers k such that $-N_x/2 \leq k \leq N_x/2$. At the discrete level, the usual L^2 norm in space, and the norm $L^2_{M^{-1}}$ defined in (10) will be computed using the space and velocity discretization

$$\|\rho\|^2_{L^2_{N_x}} = \Delta x \sum_{i=1}^{N_x} |\rho(x_i)|^2, \quad \|f\|^2_{L^2_{M^{-1},N_x,N_v}} = \Delta x \Delta v \sum_{i=1}^{N_x}\sum_{j=1}^{N_v} \frac{|f(x_i,v_j)|^2}{M(v_j)}. \tag{32}$$

Eventually, in the following numerical tests, we will take $N_x = 32$ and consider the initial condition

$$f_{in}(x,v) = (1+\sin(\pi x))M(v). \tag{33}$$

We want our schemes to enjoy a stronger property than the AP one. Indeed, they respect the two steps of the convergence of (1) towards (5) following the diagram (9).

The peculiar asymptotic behavior of (1) comes from the effect of the high velocities in the equilibrium function M. Indeed, its heavy-tailed character makes the usual diffusion coefficient (3) be infinite. The anomalous scaling $\Theta(\varepsilon)$ is chosen to counterbalance the weight of M for large velocities. It is then necessary to take them into account in the numerical computations. One idea would be to consider an adaptive grid for large velocities, to use as much large velocities as needed. However, linking the stiffness ε and the discretization parameters is not in the spirit of AP strategies. We propose a method based on analytical modifications of the terms degenerating into (8) in the schemes. These modifications are done consistently in the schemes, and (8) is carefully discretized to ensure the degeneracy to the limit equation (5). Once it is done, we are able to prove that the schemes respect the asymptotic behavior of (1).

3.1. **Discretization of a_ε.** Since the degeneracy of (1) to the diffusion limit (5) goes through the equation (7), it is necessary to handle the degeneracy of (7) to (5) numerically to design AP schemes for (1). In Fourier variable, both (5) and (7) are differential equations, which can be solved analytically, and that can also be solved with classical schemes. For instance, a semidiscrete-in-time implicit scheme for (7) reads

$$\frac{\hat{\tilde{\rho}}_\varepsilon^{n+1} - \hat{\tilde{\rho}}_\varepsilon^{n}}{\Delta t} + a_\varepsilon(k)\hat{\tilde{\rho}}_\varepsilon^{n+1} = 0, \tag{34}$$

and it degenerates into a scheme solving (5) if $a_\varepsilon(k) \to a_0(k) = mc_d|k|^2$ when ε goes to 0. If the velocity integrations are done continuously, this is ensured thanks to (13). Unfortunately, the discrete velocity integration breaks this property. Indeed, with (29) the discrete version of $a_\varepsilon(k)$ writes

$$\begin{aligned}\frac{1}{\Theta(\varepsilon)}\left\langle \frac{\varepsilon^2k^2v^2}{1+\varepsilon^2k^2v^2}M\right\rangle_{N_v} &= \frac{\Delta v}{1+|\ln(\varepsilon)|}\sum_{j=1}^{N_v}\frac{k^2v_j^2}{1+\varepsilon^2k^2v_j^2}M(v_j) \\ &\underset{\varepsilon\to 0}{\sim} \frac{\Delta v}{1+|\ln(\varepsilon)|}\sum_{j=1}^{N_v}k^2v_j^2M(v_j).\end{aligned} \tag{35}$$

Since the quadrature uses a finite number of points, the sum above is finite whilst its continuous version is infinite. Then, the naive numerical version of $a_\varepsilon(k)$ tends to 0 when $\varepsilon \to 0$, which is not satisfactory. Consequently, it is necessary to modify analytically a_ε before applying the discretization (29), to ensure the correct asymptotic behavior of a_ε. In Remark 1, the expressions $a_\varepsilon(k)$ rewritten in (20)-(21)-(22) make the limit behavior of a_ε clearly appear. Hence, at the discrete level, we rather use a discrete version of these terms, where the integrals are computed with an usual quadrature (29). It ensures the discrete version $a_\varepsilon^{N_v}$ of a_ε to degenerate to the expected diffusion coefficient when ε tends to 0. To do so, in dimension 1, we

use the following discrete version of a_ε, from (20)

$$a_\varepsilon^{N_v}(k) = \begin{cases} \dfrac{m}{1+|\ln(\varepsilon)|} & \left\langle \dfrac{k^2v^2}{1+\varepsilon^2k^2v^2} \right\rangle_{N_v,|v|\leq 1} \\ & +2m|k|^2\left(1+\dfrac{\frac{1}{2}\ln\left(\varepsilon^2+\frac{1}{|k|^2}\right)-1}{1+|\ln(\varepsilon)|}\right), \quad k\neq 0 \\ 0, & k=0, \end{cases} \tag{36}$$

which respects the estimates (13) at the discrete level. Eventually, with $a_\varepsilon^{N_v}$, the Euler scheme for (7) degenerates when ε goes to 0, to a Euler scheme for (5).

The numerical tests highlight this behavior. Indeed, Fig. 1 displays the solutions given by the scheme (34), with a_ε computed with the discretizations (35) and (36). The solutions are computed with $\Delta t = 10^{-2}$, for a range of ε. We also plot the numerical solution of the limit model approximated by

$$\frac{\hat\rho_0^{n+1}-\hat\rho_0^n}{\Delta t} + 2m|k|^2\hat\rho_0^{n+1} = 0. \tag{37}$$

When a_ε is computed directly with (35), we observe that the solution of (34) does not tend to the limit diffusion when ε goes to 0, but to the initial condition $\rho_{in} = \langle f_{in}\rangle_{N_v}$, with f_{in} defined in (33). Conversely, the solution of (34) with a_ε computed with (36), comes close to the solution of (37) when ε goes to 0. Moreover, Fig. 2 suggests that this convergence in ε happens with the speed $1/(1+|\ln(\varepsilon)|)$, proved in Prop. 2. To obtain this figure, we computed the solution $\rho_{\varepsilon,\Delta t}$ of (34) with (36), and the solution $\rho_{\Delta t}$ of (37), with $\Delta t = 10^{-2}$. Then, we plotted the relative error

$$Error(\varepsilon) = \frac{\|\rho_{\varepsilon,\Delta t}-\rho_{\Delta t}\|_{L^2_{N_x}}}{\|\rho_{\Delta t}\|_{L^2_{N_x}}},$$

with $\|\cdot\|_{L^2_{N_x}}$ defined in (32), as a function of $\varepsilon\in(0,1)$.

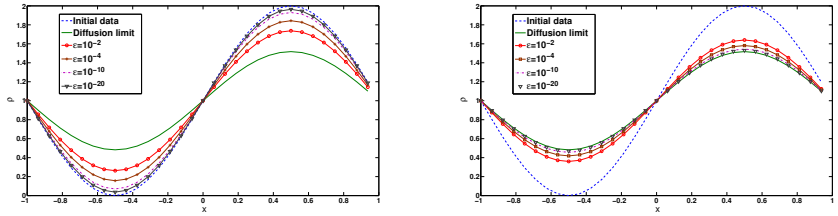

FIGURE 1. For $\Delta t = 10^{-2}$, the solutions of (37) and (34) at time $T = 0.1$ for different values of ε. Left: when a_ε is computed with (35). Right: when a_ε is computed with (36).

3.2. **Implicit scheme (IS).** The first idea to write a scheme for (1) which enjoys the AP property is to use a fully implicit scheme for (1) written in Fourier variable. Indeed, it is well-known that in the case of the classical diffusion limit, such a scheme degenerates when $\varepsilon\to 0$ into a scheme solving the limit equation. In our case, such an approach does not work, due to the effects of large velocities. Then, it is necessary to suitably write the scheme to make this degeneracy appear. We

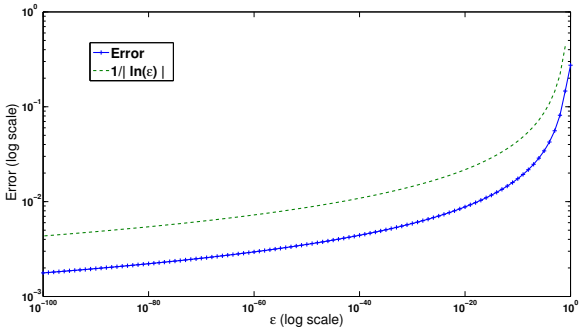

FIGURE 2. For $\Delta t = 10^{-2}$, the relative error between the solution of the scheme (34) and the limit scheme (37) at time $T = 0.1$, in function of ε (log scale).

start with (1) written in space Fourier variable, and we consider a fully implicit time discretization

$$\frac{\hat{f}^{n+1} - \hat{f}^n}{\Delta t} + \frac{1}{\Theta(\varepsilon)} \left(1 + \mathrm{i}\varepsilon k \cdot v\right) \hat{f}^{n+1} = \frac{1}{\Theta(\varepsilon)} \hat{\rho}^{n+1} M, \tag{38}$$

where the dependence in ε of f^{n+1}, f^n and ρ^{n+1} has been omitted to simplify the notations. This scheme degenerates when $\varepsilon \to 0$ into

$$\hat{f}^{n+1} = \hat{\rho}^{n+1} M.$$

Therefore, provided that the density $\hat{\rho}^{n+1}$ is known, the scheme (38) enjoys the AP property, and $\hat{f}^{n+1}$ reads

$$\hat{f}^{n+1} = \frac{\Theta(\varepsilon)\hat{f}^n + \Delta t\ \hat{\rho}^{n+1} M}{\Theta(\varepsilon) + \Delta t + \mathrm{i}\varepsilon \Delta t\ k \cdot v}. \tag{39}$$

An expression for $\hat{\rho}^{n+1}$ is given by a fully implicit time discretization of (1) integrated in velocity

$$\frac{\hat{\rho}^{n+1} - \hat{\rho}^n}{\Delta t} + \frac{1}{\Theta(\varepsilon)} \left\langle \mathrm{i}\varepsilon k \cdot v \hat{f}^{n+1} \right\rangle = 0,$$

which writes, using the expression of $\hat{f}^{n+1}$ in (39)

$$\frac{\hat{\rho}^{n+1} - \hat{\rho}^n}{\Delta t} + \left\langle \frac{\mathrm{i}\varepsilon k \cdot v \hat{f}^n}{\Theta(\varepsilon) + \Delta t + \mathrm{i}\Delta t \varepsilon k \cdot v} \right\rangle + \frac{\Delta t}{\Theta(\varepsilon)} \left\langle \frac{\mathrm{i}\varepsilon k \cdot v M}{\Theta(\varepsilon) + \Delta t + \mathrm{i}\varepsilon \Delta t k \cdot v} \right\rangle \hat{\rho}^{n+1} = 0. \tag{40}$$

Using the symmetry of M, the last term of the previous expression can be rewritten as

$$\frac{\Delta t}{\Theta(\varepsilon)}\left\langle \frac{\mathrm{i}\varepsilon k\cdot vM}{\Theta(\varepsilon)+\Delta t+\mathrm{i}\varepsilon\Delta t k\cdot v}\right\rangle \hat{\rho}^{n+1}$$

$$=\frac{\Delta t^2}{\Theta(\varepsilon)}\left\langle \frac{\varepsilon^2(k\cdot v)^2}{\left(\Theta(\varepsilon)+\Delta t\right)^2+\varepsilon^2\Delta t^2\left(k\cdot v\right)^2}M\right\rangle \hat{\rho}^{n+1} \tag{41}$$

$$=\frac{1}{\Theta(\varepsilon)}\left\langle \frac{\varepsilon^2\left(k\cdot v\right)^2}{\left(\frac{\Theta(\varepsilon)+\Delta t}{\Delta t}\right)^2+\varepsilon^2\left(k\cdot v\right)^2}M\right\rangle \hat{\rho}^{n+1}. \tag{42}$$

The expression (41) indicates that the term is of order Δt^2 for fixed ε, and thus can be removed or modified with no incidence on the accuracy of the scheme. The expression (42) shows that it degenerates into the coefficient $a_\varepsilon(k)$ when ε decreases. Since the second term of (40) vanishes for small ε, if the integrations in velocity are done continuously, the scheme degenerates when ε to 0 into a scheme solving (7). To ensure the AP property at the fully discrete level, (42) can be approximated by

$$\left(\frac{\Delta t}{\Theta(\varepsilon)+\Delta t}\right)^2\frac{1}{\Theta(\varepsilon)}\left\langle \frac{\varepsilon^2(k\cdot v)^2}{1+\varepsilon^2(k\cdot v)^2}M\right\rangle \hat{\rho}^{n+1/2}=\left(\frac{\Delta t}{\Theta(\varepsilon)+\Delta t}\right)^2 a_\varepsilon(k)\hat{\rho}^{n+1/2},$$

where $\hat{\rho}^{n+1/2}$ can be taken equal to $\hat{\rho}^n$ or $\hat{\rho}^{n+1}$, depending on the desired limit scheme (implicit or explicit). Then the coefficient a_ε is numerically approximated as in Section 3.1 to ensure the AP property. Eventually, we have the following proposition

Proposition 4. *We consider the following scheme defined for all k and all time indices $0\le n\le N, N\Delta t=T$ by*

$$\begin{cases} \dfrac{\hat{f}^{n+1}-\hat{f}^n}{\Delta t}+\dfrac{1}{\Theta(\varepsilon)}\left(1+\mathrm{i}\varepsilon k\cdot v\right)\hat{f}^{n+1}=\dfrac{1}{\Theta(\varepsilon)}\hat{\rho}^{n+1}M \\ \dfrac{\hat{\rho}^{n+1}-\hat{\rho}^n}{\Delta t}+\left\langle \dfrac{\mathrm{i}\varepsilon k\cdot v\hat{f}^n}{\Theta(\varepsilon)+\Delta t+\mathrm{i}\Delta t\varepsilon k\cdot v}\right\rangle_{N_v}+\left(\dfrac{\Delta t}{\Delta t+\Theta(\varepsilon)}\right)^2 a_\varepsilon^{N_v}(k)\hat{\rho}^{n+1/2}=0, \end{cases} \tag{43}$$

with $\Theta(\varepsilon)$ and $a_\varepsilon^{N_v}$ defined in (6) and (36), and with initial condition $\hat{f}^0(k,v)=\hat{f}_{in}(k,v), \hat{\rho}^0(k)=\left\langle \hat{f}^0(k,\cdot)\right\rangle_{N_v}$. The quantity $\hat{\rho}^{n+1/2}$ can be chosen equal to $\hat{\rho}^n$ or $\hat{\rho}^{n+1}$ depending on the desired asymptotic scheme (implicit or explicit in time). This scheme has the following properties:

1. *The scheme is of order 1 for fixed $\varepsilon>0$ and preserves the total mass.*
2. *The scheme is AP: for a fixed Δt, the scheme solves the diffusion equation (5) when ε goes to 0*

$$\frac{\hat{\rho}^{n+1}-\hat{\rho}^n}{\Delta t}+mc_d|k|^2\hat{\rho}^{n+1/2}=0, \tag{44}$$

with $c_1=2, c_2=\pi, c_3=\frac{8\pi}{3}$ and where m has been defined in (4).

Remark 2. The degeneracy of (43) to a scheme solving (5) respects the two dynamics discussed in the diagram (9). Indeed, the numerical tests show that (43) degenerates with speed $\varepsilon\sqrt{1+|\ln(\varepsilon)|}$ to

$$\frac{\hat{\rho}^{n+1}-\hat{\rho}^n}{\Delta t}+a_\varepsilon^{N_v}(k)\hat{\rho}^{n+1/2}=0, \tag{45}$$

which solves (7). Then letting ε going to 0 in the previous scheme makes it degenerate to (44) with speed $1/(1+|\ln(\varepsilon)|)$.

Proof. The first point of Prop. 4 is a direct consequence of the fact that we used an Euler scheme for (1), and that the modifications we applied to it were done consistently. Taking $k=0$ in the second line of (43) yields the conservation of the total mass. Eventually, with the modification of the term (42), the AP character is straightforward. Indeed, letting ε becomes small with fixed Δt in (43) leads to

$$\begin{cases} \hat{f}^{n+1} = \hat{\rho}^{n+1} M \\ \dfrac{\hat{\rho}^{n+1} - \hat{\rho}^n}{\Delta t} + a_\varepsilon^{N_v}(k)\hat{\rho}^{n+1/2} = 0, \end{cases}$$

which degenerates into a scheme solving (5) when $\varepsilon \to 0$. □

3.3. **Micro-macro scheme (MMS).** In the previous part, we proposed an implicit scheme for (1), which has the same behavior as the solution of (1) when ε goes to 0. However, the use of the Fourier variable may be restrictive in some cases, and its extension to more general collision operators seems difficult. Moreover, the implicit treatment of the transport operator induces high computational cost, especially in multi-dimensional cases. We propose here a scheme based on a micro-macro decomposition of the distribution function f_ε, which respects the behavior of f_ε when $\varepsilon \to 0$. It treats the transport terms explicitly, and can be extended to the case of general collision operators of [27] with a strategy similar to [24].

Denoting $\rho_\varepsilon = \langle f_\varepsilon \rangle$, we consider the decomposition $f_\varepsilon(t,x,v) = \rho_\varepsilon(t,x)M(v) + g_\varepsilon(t,x,v)$, such that $\langle g_\varepsilon \rangle = 0$. Inserting it in (1) and integrating in velocity gives

$$\partial_t \rho_\varepsilon + \frac{\varepsilon}{\Theta(\varepsilon)} \langle v \cdot \nabla_x g_\varepsilon \rangle = 0. \tag{46}$$

Then, we multiply (46) by M and we subtract it from (1) to get an equation for g_ε

$$\partial_t g_\varepsilon + \frac{\varepsilon}{\Theta(\varepsilon)} v \cdot \nabla_x \rho_\varepsilon M + \frac{\varepsilon}{\Theta(\varepsilon)} \left(v \cdot \nabla_x g_\varepsilon - \langle v \cdot \nabla_x g_\varepsilon \rangle M \right) = -\frac{1}{\Theta(\varepsilon)} g_\varepsilon. \tag{47}$$

A semi-discrete-in-time numerical scheme can be designed following [26], in which we implicit the stiffest terms

$$\begin{cases} \dfrac{g^{n+1} - g^n}{\Delta t} + \dfrac{\varepsilon}{\Theta(\varepsilon)} v \cdot \nabla_x \rho^n M + \dfrac{\varepsilon}{\Theta(\varepsilon)} \left(v \cdot \nabla_x g^n - \langle v \cdot \nabla_x g^n \rangle M \right) = -\dfrac{1}{\Theta(\varepsilon)} g^{n+1} \\ \dfrac{\rho^{n+1} - \rho^n}{\Delta t} + \dfrac{\varepsilon}{\Theta(\varepsilon)} \left\langle v \cdot \nabla_x g^{n+1} \right\rangle = 0. \end{cases} \tag{48}$$

Here, the dependence in ε of ρ^n and g^n is omitted to simplify the notations. For fixed ε, it is a consistent scheme, it remains to check wether it preserves the correct asymptotic. With the first line of (48), $g^{n+1} = O(\varepsilon)$ when Δt is fixed, and then $g^{n+1} = -\varepsilon v \cdot \nabla_x \rho^n M + o(\varepsilon)$. When reported in the second line of (48), this gives the following limit scheme for ρ

$$\frac{\rho^{n+1} - \rho^n}{\Delta t} - \frac{1}{1+|\ln(\varepsilon)|} \langle v \cdot \nabla_x \left(v \cdot \nabla_x \rho^n M \right) \rangle = 0, \tag{49}$$

which does not corresponds to the expected diffusion limit. Indeed, the term into brackets is infinite when the integration in velocity is done continuously, but it is finite when the discretization (29) is applied. Hence, in this latter case, when $\varepsilon \to 0$, the limit scheme is $\rho^{n+1} = \rho^n$, which is not consistent with (5). It is then necessary

to modify (48) to ensure the correct asymptotic behavior. To do so, we modify the macro equation by making appear the inverse of the transport operator. We first remark that $\langle v\cdot\nabla_x g^{n+1}\rangle = \langle v\cdot\nabla_x f^{n+1}\rangle$, we then use a semi discrete implicit formulation of f as in the previous part (see (38) for instance)

$$f^{n+1} = \frac{\Theta(\varepsilon)}{\Theta(\varepsilon)+\Delta t}\left(I+\frac{\Delta t}{\Theta(\varepsilon)+\Delta t}\varepsilon v\cdot\nabla_x\right)^{-1} f^n + \frac{\Delta t}{\Theta(\varepsilon)+\Delta t}\left(I+\frac{\Delta t}{\Theta(\varepsilon)+\Delta t}\varepsilon v\cdot\nabla_x\right)^{-1}\rho^{n+1}M.$$

This expression is injected in the flux of the macro equation of (48) to get

$$\frac{\rho^{n+1}-\rho^n}{\Delta t} + \frac{\varepsilon}{\Theta(\varepsilon)+\Delta t}\left\langle v\cdot\nabla_x\left(\left(I+\frac{\Delta t}{\Theta(\varepsilon)+\Delta t}\varepsilon v\cdot\nabla_x\right)^{-1} f^n\right)\right\rangle \tag{50}$$

$$+\frac{\varepsilon}{\Theta(\varepsilon)}\frac{\Delta t}{\Theta(\varepsilon)+\Delta t}\left\langle v\cdot\nabla_x\left(\left(I+\frac{\Delta t}{\Theta(\varepsilon)+\Delta t}\varepsilon v\cdot\nabla_x\right)^{-1}\rho^{n+1}M\right)\right\rangle = 0. \tag{51}$$

Since the scheme is first order in time, the bracket in (50) can be simplified consistently in $\langle v\cdot\nabla_x f^n\rangle$ to avoid the inversion of a differential operator. For the same reason, we could remove (51) with no incidence on the consistency of the scheme; however, it degenerates when $\varepsilon\to 0$ to the diffusion of (5). Therefore, this term is kept to ensure the AP property of the scheme, but it must be treated with care to take correctly the effects of the high velocities into account. In Fourier variable, and using the evenness of M, (51) reads

$$\frac{1}{\Theta(\varepsilon)}\left(\frac{\Delta t}{\Theta(\varepsilon)+\Delta t}\right)^2\left\langle\frac{\varepsilon^2(k\cdot v)^2}{1+\left(\frac{\Delta t}{\Theta(\varepsilon)+\Delta t}\right)^2\varepsilon^2(k\cdot v)^2}M\right\rangle\hat\rho^{n+1}.$$

This term is of order Δt^2 when ε is fixed, and it degenerates to $a_\varepsilon(k)\hat\rho^{n+1}$ (with a_ε defined in (8)) when ε becomes small with Δt fixed. Thus, (51) can be modified consistently in $\Delta t^2/(\Theta(\varepsilon)+\Delta t)^2 a_\varepsilon(k)\hat\rho^{n+1/2}$, which ensures both the AP character of the scheme, and the fact that the numerical solution solves (7) when ε belongs to the intermediate regime in which the solution f_ε of (1) solves (7). Here, $\hat\rho^{n+1/2}$ can be chosen equal to $\hat\rho^n$ or $\hat\rho^{n+1}$.

The passage from the semi-discrete-in-time scheme to the fully discretized scheme can then be done with the quadrature (29), and the suitable discretization of a_ε defined in (8), as in section 3.1. The derivatives in space are treated with a classical first order upwind scheme; for a sake of simplicity in the notations, we still write here the spatial derivatives as continuous. Eventually, we have the following proposition.

Proposition 5. *We consider the following scheme (discretized in time and velocity) defined for all $x\in\mathbb{R}^d$, $v_j, 1\le j\le N_v$ and all time indices $0\le n\le N, N\Delta t = T>0$ by*

$$\begin{cases} \dfrac{g^{n+1}-g^n}{\Delta t} + \dfrac{\varepsilon}{\Theta(\varepsilon)}v\cdot\nabla_x\rho^n M + \dfrac{\varepsilon}{\Theta(\varepsilon)}\left(v\cdot\nabla_x g^n - \langle v\cdot\nabla_x g^n\rangle_{N_v} M\right) = -\dfrac{g^{n+1}}{\Theta(\varepsilon)} \\ \dfrac{\rho^{n+1}-\rho^n}{\Delta t} + \dfrac{\varepsilon}{\Theta(\varepsilon)+\Delta t}\langle v\cdot\nabla_x g^n\rangle_{N_v} + \left(\dfrac{\Delta t}{\Theta(\varepsilon)+\Delta t}\right)^2\mathcal{F}^{-1}\left(a_\varepsilon^{N_v}\hat\rho^{n+1/2}\right) = 0, \end{cases} \tag{52}$$

with $\Theta(\varepsilon)$ and $a_\varepsilon^{N_v}$ defined in (6) and in (36), where $\mathcal{F}^{-1}$ denotes the inverse of the Fourier transform, and with initial condition $\rho^0 = \langle f_{in}\rangle_{N_v}$, and $g^0 = f_{in} - \rho^0 M$. The quantity $\hat\rho^{n+1/2}$ can be chosen equal to $\hat\rho^n$ or $\hat\rho^{n+1}$ depending on the desired asymptotic scheme (implicit or explicit in time). This scheme has the following properties:

1. *The scheme is of first order in time for any fixed $\varepsilon > 0$ and preserves the total mass.*
2. *The scheme is AP: for a fixed Δt, the scheme solves the diffusion equation (5) when ε goes to 0*

$$\frac{\hat\rho^{n+1} - \hat\rho^n}{\Delta t} + mc_d|k|^2\hat\rho^{n+1/2} = 0, \tag{53}$$

with $c_1 = 2, c_2 = \pi, c_3 = \frac{8\pi}{3}$, and where m has been defined in (4).

Remark 3. As in the case of the implicit scheme, this scheme enjoys a property stronger than being AP, since it respects the diagram (9). Hence, it respects the dynamics of the convergence to the solution of the diffusion equation (5) when $\varepsilon \to 0$. Indeed, the numerical tests show that (52) degenerates with speed $\varepsilon\sqrt{1+|\ln(\varepsilon)|}$ to the scheme (45), which solves (7). The degeneracy to the limit scheme (53) happens much more slowly, with speed $1/(1+|\ln(\varepsilon)|)$.

Remark 4. If we want to avoid the use of Fourier variable, we can replace $\mathcal{F}^{-1}\left(a_\varepsilon^{N_v}\hat\rho^{n+1/2}\right)$ by $-mc_d\Delta_x\rho^{n+1/2}$. This modification is consistent with (1), and still enjoys the AP property, but the convergence to the limit scheme does not make a scheme for (7) arise in the intermediate regime in ε.

Proof. Since the first point comes immediately from the derivation of the scheme, let us prove the second point. The first line of (52) gives that $g^{n+1} = o(1)$ when $\varepsilon \to 0$. Once injected in the second line, it yields

$$\frac{\rho^{n+1} - \rho^n}{\Delta t} + \mathcal{F}^{-1}\left(a_\varepsilon^{N_v}\hat\rho^{n+1/2}\right) = o(1),$$

which is a consistent approximation of (7). Finally, $a_\varepsilon^{N_v}$ tends to $mc_d|k|^2$ when $\varepsilon \to 0$, which concludes the proof. □

3.4. **Integral formulation based scheme (DS).** In the previous parts, we proposed two numerical schemes solving (1), which in addition respect the asymptotic behavior of the continuous solution when ε goes to 0. They enjoy the AP property, but their precision is not uniform in ε. In this section, we propose a scheme based on an integral formulation of (1) in Fourier variable. This approach was investigated in [11]-[12] in the case of the fractional diffusion limit. This scheme was shown to be uniformly accurate (UA) : its precision does not depend on the stiffness parameter ε. A similar strategy is performed here, to deal with the diffusion case with an anomalous scaling.

We start from the Duhamel form for $\hat f_\varepsilon$, solution of (1) in space Fourier variable

$$\hat f_\varepsilon(t,k,v) = A_0(t,k,v) + \int_0^{\frac{t}{\Theta(\varepsilon)}} \mathrm{e}^{-s(1+\mathrm{i}\varepsilon k\cdot v)}\hat\rho_\varepsilon(t-\Theta(\varepsilon)s,k)M(v)\mathrm{d}s,$$

where

$$A_0(t,k,v) = \mathrm{e}^{-t(1+\mathrm{i}\varepsilon k\cdot v)}\hat f_{in}(k,v). \tag{54}$$

Evaluating at time t_{n+1} and integrating in velocity, we get

$$\hat{\rho}_\varepsilon(t_{n+1},k) = \langle A_0(t_{n+1},k,\cdot)\rangle + \sum_{j=0}^{n} \int_{\frac{t_j}{\Theta(\varepsilon)}}^{\frac{t_{j+1}}{\Theta(\varepsilon)}} \left\langle \mathrm{e}^{-s(1+\mathrm{i}\varepsilon k\cdot v)} M \right\rangle \hat{\rho}_\varepsilon(t_{n+1}-\Theta(\varepsilon)s,k)\mathrm{d}s. \tag{55}$$

To write a scheme on $\hat{\rho}_\varepsilon$, we perform a quadrature of order 2 in the integral in s; we have $\forall j \in [\![0,n]\!], \forall s \in \left[\frac{t_j}{\Theta(\varepsilon)}, \frac{t_{j+1}}{\Theta(\varepsilon)}\right]$,

$$\begin{aligned}\hat{\rho}_\varepsilon(t_{n+1}-\Theta(\varepsilon)s,k) = &\left(1-\frac{\Theta(\varepsilon)s-t_j}{\Delta t}\right)\hat{\rho}_\varepsilon\left(t_{n+1}-t_j\right)\\ &+\frac{\Theta(\varepsilon)s-t_j}{\Delta t}\hat{\rho}_\varepsilon(t_{n+1}-t_{j+1})+O(\Delta t^2).\end{aligned} \tag{56}$$

Assuming that the time derivatives of $\hat{\rho}_\varepsilon$ are uniformly bounded in ε, the remainder is uniformly bounded by a term of magnitude $O\left(\Delta t^2\right)$ independently of ε. Inserting (56) in (55) yields the following scheme for $\hat{\rho}_\varepsilon$

$$\hat{\rho}^{n+1} = \langle A_0(t_{n+1},k,\cdot)\rangle + \sum_{j=0}^{n} b_j\hat{\rho}^{n-j} + c_j\hat{\rho}^{n+1-j}, \tag{57}$$

where the dependence in ε of $\hat{\rho}_\varepsilon$ has been omitted to simplify the notations. The coefficients $b_j, c_j, 0 \le j \le n$ are given by

$$\begin{aligned} b_j &= \int_{\frac{t_j}{\Theta(\varepsilon)}}^{\frac{t_{j+1}}{\Theta(\varepsilon)}} \frac{\Theta(\varepsilon)s-t_j}{\Delta t}\left\langle \mathrm{e}^{-s(1+\mathrm{i}\varepsilon k\cdot v)}M\right\rangle \mathrm{d}s\\ c_j &= \int_{\frac{t_j}{\Theta(\varepsilon)}}^{\frac{t_{j+1}}{\Theta(\varepsilon)}} \left(1-\frac{\Theta(\varepsilon)s-t_j}{\Delta t}\right)\left\langle \mathrm{e}^{-s(1+\mathrm{i}\varepsilon k\cdot v)}M\right\rangle \mathrm{d}s. \end{aligned}$$

The consistency of this scheme comes directly from its derivation, but the discretization of the integrals in velocity appearing in b_j and c_j is crucial to ensure the AP property. Indeed, as in the previous parts, their continuous limit when ε goes to 0 makes the diffusion (5) appear. But the effects of the high velocities are not captured if (29) is used. Therefore, it is necessary to modify analytically b_j and c_j before applying the velocity discretization. The velocity integration of b_j and c_j can be rewritten as

$$\begin{aligned}\left\langle \mathrm{e}^{-s(1+\mathrm{i}\varepsilon k\cdot v)}M\right\rangle = \mathrm{e}^{-s} &+ \left\langle \left(\mathrm{e}^{-s(1+\mathrm{i}\varepsilon k\cdot v)}-\mathrm{e}^{-s}\right)M\right\rangle_{|v|<1}\\ &+ \left\langle \left(\mathrm{e}^{-s(1+\mathrm{i}\varepsilon k\cdot v)}-\mathrm{e}^{-s}\right)M\right\rangle_{|v|\ge 1},\end{aligned}$$

because $\langle M\rangle = 1$. After that, the change of variables $w = \varepsilon v$ is performed in the last term to capture the high velocity effects, and the integrals in s of b_j and c_j are

computed exactly to get

$$b_j = -\mathrm{e}^{-\frac{t_{j+1}}{\Theta(\varepsilon)}} + \frac{\Theta(\varepsilon)}{\Delta t}\mathrm{e}^{-\frac{t_j}{\Theta(\varepsilon)}}\left(1-\mathrm{e}^{-\frac{\Delta t}{\Theta(\varepsilon)}}\right) + m\left\langle \mathrm{e}^{-\frac{t_{j+1}}{\Theta(\varepsilon)}} - \frac{\mathrm{e}^{-\frac{t_{j+1}}{\Theta(\varepsilon)}(1+\mathrm{i}\varepsilon k\cdot v)}}{1+\mathrm{i}\varepsilon k\cdot v}\right\rangle_{|v|<1} \tag{58}$$
$$+ \frac{\Theta(\varepsilon)}{\Delta t} m\left\langle \mathrm{e}^{-\frac{t_j}{\Theta(\varepsilon)}(1+\mathrm{i}\varepsilon k\cdot v)}\frac{1-\mathrm{e}^{-\frac{\Delta t}{\Theta(\varepsilon)}(1+\mathrm{i}\varepsilon k\cdot v)}}{(1+\mathrm{i}\varepsilon k\cdot v)^2} - \mathrm{e}^{-\frac{t_j}{\Theta(\varepsilon)}}\left(1-\mathrm{e}^{-\frac{\Delta t}{\Theta(\varepsilon)}}\right)\right\rangle_{|v|<1}$$
$$+ \varepsilon^2 m\left\langle \frac{1}{|w|^{d+2}}\left(\mathrm{e}^{-\frac{t_{j+1}}{\Theta(\varepsilon)}} - \frac{\mathrm{e}^{-\frac{t_{j+1}}{\Theta(\varepsilon)}(1+\mathrm{i}k\cdot w)}}{1+\mathrm{i}k\cdot w}\right)\right\rangle_{|w|\geq\varepsilon}$$
$$+ \frac{\Theta(\varepsilon)}{\Delta t}\varepsilon^2 m\left\langle \frac{1}{|w|^{d+2}}\mathrm{e}^{\frac{t_j}{\Theta(\varepsilon)}(1+\mathrm{i}k\cdot w)}\frac{1-\mathrm{e}^{-\frac{\Delta t}{\Theta(\varepsilon)}(1+\mathrm{i}k\cdot w)}}{(1+\mathrm{i}k\cdot w)^2}\right\rangle_{|w|\geq\varepsilon}$$
$$- \frac{\Theta(\varepsilon)}{\Delta t}\varepsilon^2 m\left\langle \frac{1}{|w|^{d+2}}\mathrm{e}^{-\frac{t_j}{\Theta(\varepsilon)}}(1-\mathrm{e}^{-\frac{\Delta t}{\Theta(\varepsilon)}})\right\rangle_{|w|\geq\varepsilon},$$

$$c_j = \mathrm{e}^{-\frac{t_j}{\Theta(\varepsilon)}} - \frac{\Theta(\varepsilon)}{\Delta t}\mathrm{e}^{-\frac{t_j}{\Theta(\varepsilon)}}\left(1-\mathrm{e}^{-\frac{\Delta t}{\Theta(\varepsilon)}}\right) \tag{59}$$
$$- \frac{\Theta(\varepsilon)}{\Delta t} m\left\langle \mathrm{e}^{-\frac{t_j}{\Theta(\varepsilon)}(1+\mathrm{i}\varepsilon k\cdot v)}\frac{1-\mathrm{e}^{-\frac{\Delta t}{\Theta(\varepsilon)}(1+\mathrm{i}\varepsilon k\cdot v)}}{(1+\mathrm{i}\varepsilon k\cdot v)^2} - \mathrm{e}^{-\frac{t_j}{\Theta(\varepsilon)}}\left(1-\mathrm{e}^{-\frac{\Delta t}{\Theta(\varepsilon)}}\right)\right\rangle_{|v|<1}$$
$$+ m\left\langle \frac{\mathrm{e}^{-\frac{t_j}{\Theta(\varepsilon)}(1+\mathrm{i}\varepsilon k\cdot v)}}{1+\mathrm{i}\varepsilon k\cdot v} - \mathrm{e}^{-\frac{t_j}{\Theta(\varepsilon)}}\right\rangle_{|v|<1}$$
$$+ \varepsilon^2 m\left\langle \frac{1}{|w|^{d+2}}\left(\frac{\mathrm{e}^{-\frac{t_j}{\Theta(\varepsilon)}(1+\mathrm{i}k\cdot w)}}{1+\mathrm{i}k\cdot w} - \mathrm{e}^{-\frac{t_j}{\Theta(\varepsilon)}}\right)\right\rangle_{|w|\geq\varepsilon} \tag{60}$$
$$- \frac{\Theta(\varepsilon)}{\Delta t}\varepsilon^2 m\left\langle \frac{1}{|w|^{d+2}}\mathrm{e}^{-\frac{t_j}{\Theta(\varepsilon)}(1+\mathrm{i}k\cdot w)}\frac{1-\mathrm{e}^{-\frac{\Delta t}{\Theta(\varepsilon)}(1+\mathrm{i}k\cdot w)}}{(1+\mathrm{i}k\cdot w)^2}\right\rangle_{|w|\geq\varepsilon}$$
$$+ \frac{\Theta(\varepsilon)}{\Delta t}\varepsilon^2 m\left\langle \frac{1}{|w|^{d+2}}\mathrm{e}^{-\frac{t_j}{\Theta(\varepsilon)}}\left(1-\mathrm{e}^{-\frac{\Delta t}{\Theta(\varepsilon)}}\right)\right\rangle_{|w|\geq\varepsilon}.$$

However, it is still not sufficient to ensure the AP character of the scheme when the integrals are discretized since, when $j=0$, the term (60) reads

$$\Theta(\varepsilon)\left(\frac{m}{1+|\ln(\varepsilon)|}\left\langle\frac{(k\cdot v)^2}{1+\varepsilon^2(k\cdot v)^2}\right\rangle_{|v|<1} + \frac{m}{1+|\ln(\varepsilon)|}\left\langle\frac{1}{|w|^{d+2}}\frac{(k\cdot w)^2}{1+(k\cdot w)^2}\right\rangle_{|w|\geq\varepsilon}\right),$$

which is equal to $\Theta(\varepsilon)a_\varepsilon$, with a_ε defined in (8) and rewritten in (15) (note that the equality (15) is valid for any dimension). In Section 3.1, we established that the discretization of this term is crucial to ensure the AP property of our schemes. Following the strategy presented previously, we then replace (60) by an appropriate

discretization $\Theta(\varepsilon)a_\varepsilon^{N_v}$ defined in (36) when $j=0$. Eventually, c_0 rewrites

$$\begin{aligned} c_0 = {} & \Theta(\varepsilon)a_\varepsilon^{N_v}(k)+1 \\ & - \frac{\Theta(\varepsilon)}{\Delta t}\left(1-\mathrm{e}^{-\frac{\Delta t}{\Theta(\varepsilon)}}\right) - \frac{\Theta(\varepsilon)}{\Delta t} m \left\langle \frac{1-\mathrm{e}^{-\frac{\Delta t}{\Theta(\varepsilon)}(1+\mathrm{i}\varepsilon k\cdot v)}}{(1+\mathrm{i}\varepsilon k\cdot v)^2} - 1 + \mathrm{e}^{-\frac{\Delta t}{\Theta(\varepsilon)}} \right\rangle_{|v|<1} \\ & - \frac{\Theta(\varepsilon)}{\Delta t} m\varepsilon^2 \left\langle \frac{1}{|w|^{d+2}} \left(\frac{1-\mathrm{e}^{-\frac{\Delta t}{\Theta(\varepsilon)}(1+\mathrm{i}k\cdot w)}}{(1+\mathrm{i}k\cdot w)^2} - 1 + \mathrm{e}^{-\frac{\Delta t}{\Theta(\varepsilon)}} \right) \right\rangle_{|w|\geq\varepsilon}. \end{aligned} \tag{61}$$

The expressions b_j $(j\geq 0)$, c_j $(j\geq 1)$ and c_0, defined in (58)-(59)-(61), computed with the discretization (29) make the scheme (57) AP. Moreover, let us remark that the scheme only uses ρ and not f. It implies that the computation of the whole distribution f is not necessary, which represents a gain of computational cost, since the problem for f is of higher dimension than the problem on ρ. Let us note that f can even so be computed in Fourier variable with a scheme similar to (57). Indeed, Duhamel formula of (1) between the times t_n and t_{n+1} leads to

$$\begin{aligned} \hat f_\varepsilon(t_{n+1},k,v) = {} & \mathrm{e}^{-\frac{\Delta t}{\Theta(\varepsilon)}(1+\mathrm{i}\varepsilon k\cdot v)}\hat f_\varepsilon(t_n,k,v) \\ & + \int_0^{\frac{\Delta t}{\Theta(\varepsilon)}} \mathrm{e}^{-s(1+\mathrm{i}\varepsilon k\cdot v)}\hat\rho_\varepsilon(t_{n+1}-\Theta(\varepsilon)s,k)M(v)\mathrm{d}s. \end{aligned} \tag{62}$$

As in the scheme for $\hat\rho$, we apply the quadrature (56) in the integral in s, and the scheme for $\hat f$ reads

$$\hat f^{n+1} = \mathrm{e}^{-\frac{\Delta t}{\Theta(\varepsilon)}(1+\mathrm{i}\varepsilon k\cdot v)}\hat f^n + \beta\hat\rho^n M + \gamma\hat\rho^{n+1}M,$$

where the dependence in ε of $\hat f$ has been omitted, and with

$$\beta = \int_0^{\frac{\Delta t}{\Theta(\varepsilon)}} \frac{\Theta(\varepsilon)s}{\Delta t}\mathrm{e}^{-s(1+\mathrm{i}\varepsilon k\cdot v)}\mathrm{d}s = -\frac{\mathrm{e}^{-\frac{\Delta t}{\Theta(\varepsilon)}(1+\mathrm{i}\varepsilon k\cdot v)}}{1+\mathrm{i}\varepsilon k\cdot v} + \frac{\Theta(\varepsilon)}{\Delta t}\frac{1-\mathrm{e}^{-\frac{\Delta t}{\Theta(\varepsilon)}(1+\mathrm{i}\varepsilon k\cdot v)}}{(1+\mathrm{i}\varepsilon k\cdot v)^2} \tag{63}$$

$$\gamma = \int_0^{\frac{\Delta t}{\Theta(\varepsilon)}} \left(1-\frac{\Theta(\varepsilon)s}{\Delta t}\right)\mathrm{e}^{-s(1+\mathrm{i}\varepsilon k\cdot v)}\mathrm{d}s = \frac{1}{1+\mathrm{i}\varepsilon k\cdot v} - \frac{\Theta(\varepsilon)}{\Delta t}\frac{1-\mathrm{e}^{-\frac{\Delta t}{\Theta(\varepsilon)}(1+\mathrm{i}\varepsilon k\cdot v)}}{(1+\mathrm{i}\varepsilon k\cdot v)^2}. \tag{64}$$

Eventually, we have the following proposition.

Proposition 6. *Provided the initial condition* $\left(\hat f^0(k,v_j)\right)_{j\in[\![1,N_v]\!]} = \left(\hat f_{in}(k,v_j)\right)_{j\in[\![1,N_v]\!]}$, $\hat\rho^0(k) = \left\langle \hat f^0(k,\cdot)\right\rangle_{N_v}$, *we consider the following scheme, defined for all k and all time indices $0\leq n\leq N, N\Delta t = T$, by*

$$\begin{cases} \hat\rho^{n+1}(k) = \dfrac{\langle A_0(t_{n+1},k,v)\rangle_{N_v} + b_0\hat\rho^n(k) + \sum_{j=1}^{n}\left[b_j\hat\rho^{n-j}(k)+c_j\hat\rho^{n+1-j}(k)\right]}{1-c_0} \\ \hat f^{n+1} = \mathrm{e}^{-\frac{\Delta t}{\Theta(\varepsilon)}(1+\mathrm{i}\varepsilon k\cdot v)}\hat f^{n+1} + \beta\hat\rho^n M + \gamma\hat\rho^{n+1}M, \end{cases} \tag{65}$$

with A_0,β,γ defined in (54)-(63)-(64), and $b_j(j\geq 0), c_j(j\geq 1)$ and c_0 defined in (58)-(59)-(61) and computed with (29). This scheme has the following properties:

1. *The scheme is first order in time and preserves the total mass.*

2. *The scheme is AP: for a fixed Δt, it solves the diffusion equation (5) when ε goes to zero*
$$\frac{\hat{\rho}^{n+1}-\hat{\rho}^n}{\Delta t}+mc_d|k|^2\hat{\rho}^{n+1}=0,$$
with $c_1=2, c_2=\pi, c_3=\frac{3\pi}{8}$, and where m has been defined in (4).
3. *Moreover, the semi-discrete-in-time scheme enjoys the UA property: it is first order uniformly in ε*
$$\exists C>0,\ \sup_{\varepsilon\in(0,1]}\|\hat{f}^N(\cdot,\cdot)-\hat{f}(T,\cdot,\cdot)\|_{L^\infty_{k,v}}\leq C\Delta t.$$

Remark 5. The UA property of the scheme ensures that it respects the dynamics of the convergence towards the diffusion equation (5).

Proof. The conservation of the mass can be proved by induction on the expression of $\hat{\rho}^{n+1}$ for $k=0$. Moreover, since the proof of the third point of Prop. 6 is very similar to the one presented in [11]-[12] in the case of the fractional diffusion limit, we just prove the AP character of the scheme (65). First of all, let us remark that A_0,b_j and c_j ($j\geq 1$) defined in (54)-(58)-(59) are exponentially small when ε goes to 0. The expressions (58) and (61) then give the following equivalents for b_0 and c_0
$$b_0=\frac{\Theta(\varepsilon)}{\Delta t}+\Theta(\varepsilon)o\left(1\right),\quad c_0=\Theta(\varepsilon)a_\varepsilon^{N_v}+\frac{\Theta(\varepsilon)}{\Delta t}+\Theta(\varepsilon)o(1).$$
Hence the scheme for $\hat{\rho}$ degenerates when ε goes to 0 into
$$\frac{\hat{\rho}^{n+1}-\hat{\rho}^n}{\Delta t}+a_\varepsilon^{N_v}\hat{\rho}^{n+1}=0.$$
The asymptotic behavior of $a_\varepsilon^{N_v}$ has already been studied, it remains to consider the limit of the expression of $\hat{f}^{n+1}$ when ε goes to 0. From (63) and (64), we have
$$\beta=O(\Theta(\varepsilon)),\quad \gamma=1+O(\Theta(\varepsilon)),$$
and eventually the scheme for $\hat{f}^{n+1}$ degenerates for small ε into $\hat{f}^{n+1}=\hat{\rho}^{n+1}M$. □

4. **Numerical tests.** In this section, we propose numerical tests in dimension 1 to validate the schemes of the previous parts. For simplicity, we will denote IS the implicit scheme of Prop. 4, MMS the micro-macro scheme of Prop. 5, and DS the integral formulation based scheme of Prop. 6. The implicit Euler scheme (45) for the equation (7), with a_ε computed with (36), will be denoted *quasi-diff*. Eventually, the scheme (44) for the limit diffusion equation (5) will be denoted *diff*. To highlight the consistency of the schemes, we will compare their solutions to the solution of a reference scheme which is an explicit Euler scheme in Fourier variable for (1)
$$\begin{cases}\dfrac{\hat{f}^{n+1}-\hat{f}^n}{\Delta t}+\dfrac{1}{\Theta(\varepsilon)}\left(1+\mathrm{i}\varepsilon kv\right)\hat{f}^n=\dfrac{1}{\Theta(\varepsilon)}\hat{\rho}^nM\\ \hat{\rho}^{n+1}=\left\langle\hat{f}^{n+1}\right\rangle_{N_v}\\ \hat{f}^0(k,v)=\hat{f}_{in}(k,v).\end{cases}\tag{66}$$
As detailed in the beginning of Section 3, all the tests are performed at time $T=0.1$, the time step being specified in each case. We will consider N_x points in space on the interval $[-1,1]$ with periodic boundary conditions, and the velocities are discretized with $N_v=199$ points symmetrically distributed on the interval $[-10,10]$. The initial

condition is (33). In the DS scheme, the velocity integrations with the variable w in (58)-(59)-(61) are computed with the same grid as the integrals with the v variable.

4.1. **Implicit scheme (IS).** In this section, we test the properties of the IS scheme. First of all, its consistency is tested. The left part of Fig. 3 shows that, for $\varepsilon = 1$, its solution coincides with the solution of the explicit scheme (66). For this figure, the two solutions are computed with the time step $\Delta t = 10^{-2}$. Then, the solution $\rho_{\Delta t}$ of the IS scheme for a range of Δt is compared to the solution $\rho_{\Delta t_{ref}=10^{-6}}$ of the IS scheme for $\Delta t_{ref} = 10^{-6}$ at time $T = 0.1$. The relative error between these densities

$$\text{Error}_{\text{consistency}}(\Delta t, \varepsilon) = \frac{\|\rho_{reference} - \rho_{\Delta t}\|_{L^2_{N_x}}}{\|\rho_{reference}\|_{L^2_{N_x}}}, \tag{67}$$

with $\|\cdot\|_{L^2_{N_x}}$ defined in (32), is displayed in the right-hand side of Fig. 3 in function of Δt. As it is a line with slope 0.98, the numerical order of the method is 1.

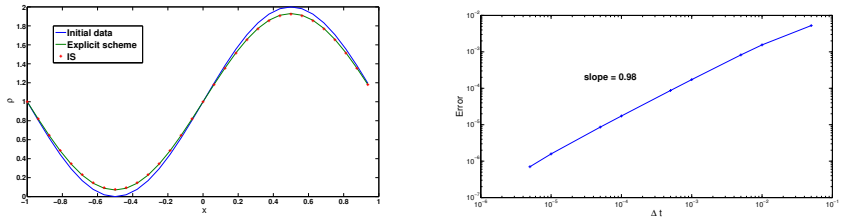

FIGURE 3. Left: for $\Delta t = 10^{-2}$ and $\varepsilon = 1$, the solutions of the IS scheme and of the explicit scheme (66). Right: The relative consistency error (67) for the IS scheme (log scale).

Then, the AP character of the IS scheme is tested. The dynamics of the convergence towards the diffusion limit (5) is highlighted in the left part of Fig. 4, where the densities obtained with the IS scheme are presented for a range of ε, and compared to the densities given by *quasi-diff* and *diff* schemes. These solutions are computed with $\Delta t = 10^{-2}$. For intermediate ε, the solution of the IS scheme sticks to the solution of *quasi-diff*, and the two densities goes together to the solution of *diff* when ε tends to 0. The convergence towards the solution of *quasi-diff* happens with speed $\varepsilon\sqrt{1 + |\ln(\varepsilon)|}$, as suggested by the error study presented in the right-hand side of Fig. 4. Denoting by f the distribution function obtained with the IS scheme, and $\rho_{quasi-diff}$ the density obtained with the *quasi-diff* scheme for $\Delta t = 10^{-2}$, the quantity

$$\text{Error}_{\text{AP}}(\varepsilon) = \|f - \rho_{quasi-diff} M\|_{L^2_{M^{-1},N_x,N_v}}, \tag{68}$$

with $\|\cdot\|_{L^2_{M^{-1},N_x,N_v}}$ defined in (32), is displayed in function of ε. This numerical quantity decreases with the expected rate $\varepsilon\sqrt{1 + |\ln(\varepsilon)|}$ stated in Prop. 1. Note that the numerical results of section 3.1 assure that the convergence of the solution of IS to the solution of *diff* happens with the speed $1/(1 + |\ln(\varepsilon)|)$ proved in Prop. 2.

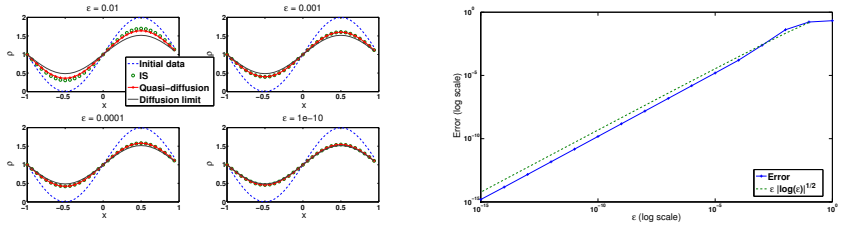

FIGURE 4. Left: for $\Delta t = 10^{-2}$, the solutions of IS, *quasi-diff* and *diff* schemes for different values of ε. Right: for $\Delta t = 10^{-2}$, the error (68) between the solution of IS and *quasi-diff* scheme in function of ε (log scale).

4.2. **Micro-macro scheme (MMS).** In this section, we focus on the MMS scheme and we highlight its properties with the same tests as in the previous section. As the transport operator is treated with a classical upwind scheme in the MMS scheme, the CFL condition imposes to take time steps smaller than in the previous section. The left-hand side of Fig. 5 shows that the solutions of the MMS and explicit schemes with $\Delta t = 10^{-4}$ and $\varepsilon = 1$ coincide. The numerical order of the MMS scheme is studied in the right-hand side of Fig. 5, where the consistency error (67) for $\varepsilon = 1$ is displayed in function of Δt. For this figure, the density $\rho_{reference}$ is the density obtained with the MMS scheme for $\Delta t = 10^{-6}$ and $\rho_{\Delta t}$ are densities obtained with the MMS scheme for a range of Δt. As expected, the numerical order of the method is 1.

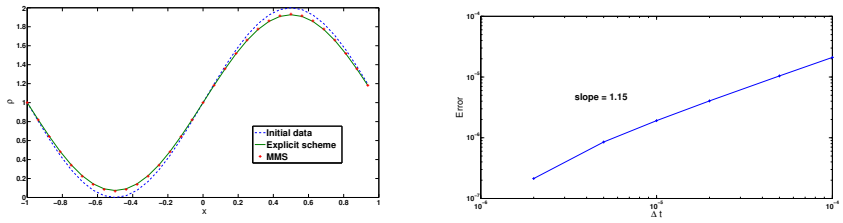

FIGURE 5. Left: for $\Delta t = 10^{-4}$ and $\varepsilon = 1$, the solutions of the MMS scheme and of the explicit scheme (66). Right: The relative consistency error (67) for the MMS scheme (log scale).

Concerning the AP character of the MMS scheme, the left-hand side of Fig. 6 shows, for a range of ε, the densities obtained with the MMS, *quasi-diff* and *diff* schemes with $\Delta t = 10^{-4}$. Once again, the solution of the MMS scheme first joins the solution of the *quasi-diff* scheme when ε becomes small and the two reach the solution of *diff* scheme together when ε tends to 0. The speed of the convergence towards the solution of *quasi-diff* scheme is $\varepsilon\sqrt{1+|\ln(\varepsilon)|}$ stated in Prop. 1. Indeed, the right-hand side of Fig. 6 displays the error (68), where $\rho_{quasi-diff}$, and the solution f given by the MMS scheme are computed with $\Delta t = 10^{-4}$.

4.3. **Integral formulation based scheme (DS).** In this section, we test the integral formulation scheme DS. For $\varepsilon = 1$, we check in the left-hand side of Fig.

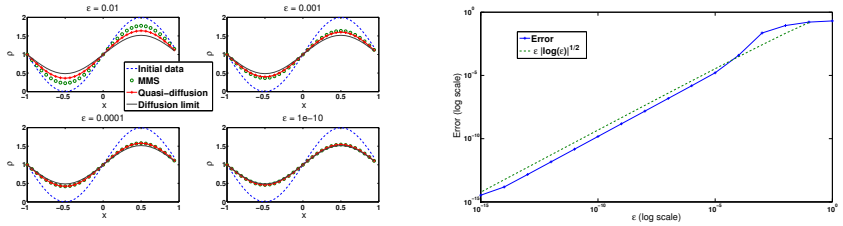

FIGURE 6. Left: for $\Delta t = 10^{-4}$, the solutions of MMS, *quasi-diff* and *diff* schemes for different values of ε. Right: for $\Delta t = 10^{-4}$, the error (68) between the solution of MMS and *quasi-diff* scheme in function of ε (log scale).

7, that the solutions of the explicit and DS schemes are close. This figure was obtained with $\Delta t = 10^{-2}$. The order of accuracy of the DS scheme is studied in the right-hand side of Fig. 7. For $\varepsilon = 1$, it displays the error (67) between $\rho_{reference}$ defined as the solution of the DS scheme for $\Delta t = 5 \cdot 10^{-5}$, and the solution of the DS scheme $\rho_{\Delta t}$ for a range of Δt. In a logarithmic scale, the slope of the line obtained is close to 1, as expected.

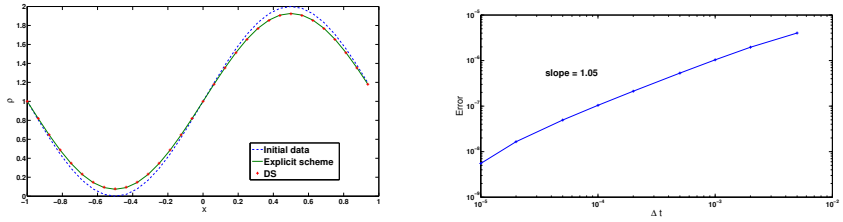

FIGURE 7. Left: for $\Delta t = 10^{-2}$ and $\varepsilon = 1$, the solutions of the DS scheme and of the explicit scheme (66). Right: The relative consistency error (67) for the DS scheme (log scale).

Then, we can study the AP character of the DS scheme. The dynamics of the convergence towards the diffusion limit (5) is highlighted in the left-hand side of Fig. 8. It presents the densities obtained with the DS, *quasi-diff* and *diff* schemes for $\Delta t = 10^{-2}$. The solution of the DS scheme has the right behavior, since it is very close to the solution of *quasi-diff* for intermediate ε, and remains stuck to it as it goes to the solution of *diff* when ε goes to 0. The right-hand side of Fig. 8 displays the error study of the convergence in ε of the solution of the DS scheme to the solution of the *quasi-diff* scheme. The error (68) is displayed in a logarithmic scale in this figure, where both $\rho_{quasi-diff}$ and the solution f of the DS scheme are computed with $\Delta t = 10^{-2}$. The convergence happens with the expected $\varepsilon\sqrt{1 + |\ln(\varepsilon)|}$ rate.

To highlight the fact that the DS scheme is of order 1 uniformly in ε, we compare the results given by the DS scheme for $\Delta t_{ref} = 5 \cdot 10^{-5}$ to the results given by the same DS scheme for different values of Δt and ε. With these densities, the error (67) is displayed in Fig. 9 as a function of ε. We observe that the error curves are stratified with respect to ε, showing the uniformity of the scheme with respect to ε.

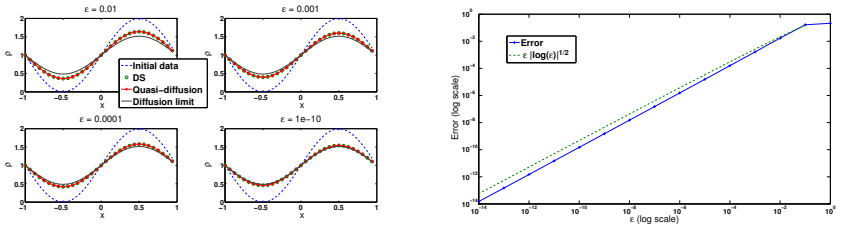

FIGURE 8. Left: for $\Delta t = 10^{-2}$, the solutions of DS, *quasi-diff* and *diff* schemes for different values of ε. Right: for $\Delta t = 10^{-2}$, the error (68) between the solution of DS and *quasi-diff* scheme in function of ε (log scale).

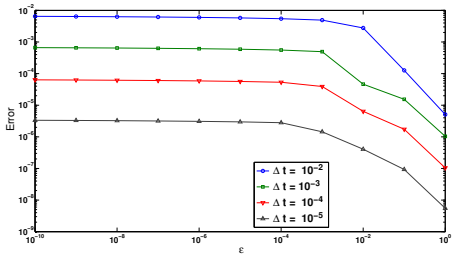

FIGURE 9. The error (67) as a function of ε. The density $\rho_{reference}$ is the density given by the DS scheme for $\Delta t_{ref} = 5 \cdot 10^{-5}$, and $\rho_{\Delta t}$ are the densities given by the DS scheme for different values of Δt (log scale).

5. **Conclusion.** In this paper, we presented three AP schemes for a kinetic equation with a diffusion limit and an anomalous time scale We first proved that the convergence of the solution of the kinetic equation towards the solution of the asymptotic model happens with a slow rate in ε, but that this convergence goes through an intermediate model with a quicker convergence rate. The degeneracy $\varepsilon \to 0$ makes the problem stiff, which complicates the numerical computations, but moreover the slow rate of the convergence towards the asymptotic model makes the limit model unattainable in the numerical computations. Hence, we proposed an adaptation of the AP approach for numerical schemes, by requiring in addition the schemes to respect the dynamics of the degeneracy towards the limit equation. A second stiffness arise in the design of numerical schemes for kinetic equations with the anomalous diffusion limit we studied, since the high velocities play a crucial role in the asymptotic analysis of the model. From a numerical point of view, it is then necessary to take these high velocities correctly into account to ensure the AP property of the schemes. To deal with this stiffness, we proposed a method based on analytical transformation of the terms leading to the asymptotic model in the schemes. A similar approach was proposed in [11, 12] in the case of a fractional diffusion limit for the kinetic equation.

The first scheme we presented is based on a fully implicit discretization of the kinetic equation in Fourier variable, and the second one uses a micro-macro decomposition of the distribution function and treats the transport explicitely. Both of them enjoy the AP property and respect the dynamics of the convergence towards the limit model. The last scheme we proposed, which is based on an integral formulation of the kinetic equation in space Fourier variable, even enjoys the UA property.

In a near future, we aim at extending this work to more general context, considering an integral collision operator. In this context, the study can not be simplified by the use of the space Fourier variable. However, schemes based on a micro-macro decomposition of the distribution can be written. Moreover, the case of fractional diffusion limit of kinetic equations with an integral collision operator can also be treated with such an approach.

REFERENCES

[1] C. Bardos, F. Golse and D. Levermore, Fluid dynamic limits of kinetic equations. i. formal derivations, *J. Stat. Phys.*, **63** (1991), 323–344.

[2] C. Bardos, F. Golse and D. Levermore, Fluid dynamic limits of kinetic equations. ii: Convergence proofs for the boltzmann equations, *Comm. on Pure and Appl. Math.*, **XLVI** (1993), 667–753.

[3] C. Bardos, R. Santos and R. Sentis, Diffusion approximation and computation of the critical size, *Trans. Amer. Math. Soc.*, **284** (1984), 617–649.

[4] N. Ben Abdallah, A. Mellet and M. Puel, Fractional diffusion limit for collisional kinetic equations: A Hilbert expansion approach, *Kinet. Relat. Models*, **4** (2011), 873–900.

[5] A. Bensoussan, J.-L. Lions and G. Papanicolaou, Boundary layers and homogenization of transport processes, *Publ. Res. Int. Math. Sci.*, **15** (1979), 53–157.

[6] A. Bobylev, J. Carrillo and I. Gamba, On some properties of kinetic and hydrodynamic equations for inelastic interactions, *J. Statist. Phys.*, **98** (2000), 743–773.

[7] A. Bobylev and I. Gamba, Boltzmann equations for mixtures of Maxwell gases: Exact solutions and power like tails, *J. Statist. Phys.*, **124** (2006), 497–516.

[8] C. Buet and S. Cordier, Asymptotic preserving scheme and numerical methods for radiative hydrodynamic models, *C. R. Math. Acad. Sci. Paris*, **338** (2004), 951 – 956.

[9] J. Carrillo, T. Goudon, P. Lafitte and F. Vecil, Numerical schemes of diffusion asymptotics and moment closures for kinetic equations, *J. Sci. Comput.*, **36** (2008), 113–149.

[10] N. Crouseilles, H. Hivert and M. Lemou, Multiscale numerical schemes for kinetic equations in the anomalous diffusion limit, *C. R. Math. Acad. Sci. Paris*, **353** (2015), 755 – 760, URL http://www.sciencedirect.com/science/article/pii/S1631073X15001466.

[11] N. Crouseilles, H. Hivert and M. Lemou, Numerical schemes for kinetic equations in the anomalous diffusion limit. Part I: The case of heavy-tailed equilibrium, *SIAM, J. Sc. Comput.*, **38** (2016), A737–A764, URL http://dx.doi.org/10.1137/15M1011366.

[12] N. Crouseilles, H. Hivert and M. Lemou, Numerical schemes for kinetic equations in the anomalous diffusion limit. Part II: Degenerate collision frequency, *SIAM J. Sc. Comput.*, **38** (2016), A2464–A2491, URL http://dx.doi.org/10.1137/15M1053190.

[13] S. De Moor, Fractional diffusion limit for a stochastic kinetic equation, *Stochastic Process. Appl.*, **124** (2014), 1335 – 1367, URL http://www.sciencedirect.com/science/article/pii/S0304414913002883.

[14] S. De Moor, *Limites diffusives pour des équations cinétiques stochastiques*, PhD thesis, ENS Rennes, Rennes, France, 2014.

[15] P. Degond, T. Goudon and F. Poupaud, Diffusion limit for non homogeneous and non-micro-reversible processes, *Indiana Univ. Math. J*, **49** (2000), 1175–1198.

[16] D. del Castillo-Negrete, B. Carreras and V. Lynch, Non-diffusive transport in plasma turbulence: A fractional diffusion approach, *Phys. Rev. Lett.*, **94** (2005), 065003, URL http://link.aps.org/doi/10.1103/PhysRevLett.94.065003.

[17] M. Ernst and R. Brito, Scaling solutions of inelastic Boltzmann equations with over-populated high energy tails, *J. Statist. Phys.*, **109** (2002), 407–432.

[18] S. Jin, Efficient asymptotic-preserving (AP) schemes for some multiscale kinetic equations, *SIAM J. Sci. Comput.*, **21** (1999), 441–454.
[19] S. Jin and L. Pareschi, Discretization of the multiscale semiconductor Boltzmann equation by diffusive relaxation schemes, *J. Comput. Phys.*, **161** (2000), 312–330.
[20] S. Jin, L. Pareschi and G. Toscani, Uniformly accurate diffusive relaxation schemes for multiscale transport equations, *SIAM J. Numer. Anal.*, **38** (2000), 913–936.
[21] A. Klar, An asymptotic-induced scheme for nonstationary transport equations in the diffusive limit, *SIAM J. Numer. Anal.*, **35** (1998), 1073–1094.
[22] A. Klar, An asymptotic preserving numerical scheme for kinetic equations in the low Mach number limit, *SIAM J. Numer. Anal.*, **36** (1999), 1507–1527.
[23] C. Kleiber and S. Kotz, *Statistical size distributions in economics and actuarial sciences*, John Wiley and Sons, Hoboken, NJ, 2003.
[24] M. Lemou, Relaxed micro-macro schemes for kinetic equations, *C. R. Math. Acad. Sci. Paris*, **348** (2010), 455 – 460, URL http://www.sciencedirect.com/science/article/pii/S1631073X10000622.
[25] M. Lemou and F. Méhats, Micro-macro schemes for kinetic equations including boundary layers, *SIAM J. Sci. Comput.*, **34** (2012), 734–760, URL https://hal.archives-ouvertes.fr/hal-00751788.
[26] M. Lemou and L. Mieussens, A new asymptotic preserving scheme based on micro-macro formulation for linear kinetic equations in the diffusion limit, *SIAM J. Sci. Comput.*, **31** (2008), 334–368.
[27] A. Mellet, S. Mischler and C. Mouhot, Fractional diffusion limit for collisional kinetic equations, *Arch. Ration. Mech. Anal.*, **199** (2011), 493–525.
[28] D. A. Mendis and M. Rosenberg, Cosmic dusty plasma, *Annu. Rev. Astron. Astrophys.*, **32** (1994), 419–463.
[29] D. Summers and R. M. Thorne, The modified plasma dispersion function, *Fluids B*, **3** (1991), 1835–1847, URL http://scitation.aip.org/content/aip/journal/pofb/3/8/10.1063/1.859653.
[30] L. Wang and B. Yan, An asymptotic-preserving scheme for linear kinetic equation with fractional diffusion limit, *J. Comput. Phys.*, **312** (2016), 157 – 174, URL http://www.sciencedirect.com/science/article/pii/S002199911600098X.
[31] E. Wigner, *Nuclear reactor theory*, AMS, Providence, RI, 1961.

Received xxxx 20xx; revised xxxx 20xx.

E-mail address: helene.hivert@ens-lyon.fr